ELSEVIER

INSTITUT PASTEUR

Microbes and Infection 13 (2011) 58–64

www.elsevier.com/locate/micinf

Original article

# Improved capacity of a monkey-tropic HIV-1 derivative to replicate in cynomolgus monkeys with minimal modifications

Akatsuki Saito [a,b,c,1], Masako Nomaguchi [d,1], Sayuki Iijima [c], Ayumu Kuroishi [e], Tomoyuki Yoshida [b], Young-Jung Lee [c], Toshiyuki Hayakawa [b], Ken Kono [e], Emi E. Nakayama [e], Tatsuo Shioda [e], Yasuhiro Yasutomi [c], Akio Adachi [d], Tetsuro Matano [a], Hirofumi Akari [b,c,*]

[a] *International Research Center for Infectious Diseases, The Institute of Medical Science, The University of Tokyo, Tokyo 108-8639, Japan*
[b] *Primate Research Institute, Kyoto University, Inuyama 484-8506, Japan*
[c] *Tsukuba Primate Research Center, National Institute of Biomedical Innovation, Tsukuba 305-0843, Japan*
[d] *Department of Microbiology, Institute of Health Biosciences, The University of Tokushima Graduate School, Tokushima 770-8503, Japan*
[e] *Department of Viral Infections, Research Institute for Microbial Diseases, Osaka University, Suita 565-0871, Japan*

Received 31 July 2010; accepted 1 October 2010
Available online 16 October 2010

**Abstract**

Human immunodeficiency virus type 1 (HIV-1) hardly replicates in Old World monkeys. Recently, a mutant HIV-1 clone, NL-DT5R, in which a small part of *gag* and the entire *vif* gene are replaced with SIVmac239-derived ones, was shown to be able to replicate in pigtail monkeys but not in rhesus monkeys (RM). In the present study, we found that a modified monkey-tropic HIV-1 (HIV-1mt), MN4-5S, acquired the ability to replicate efficiently in cynomolgus monkeys as compared with the NL-DT5R, while neither NL-DT5R nor MN4-5S replicated in RM cells. These results suggest that multiple determinants may be involved in the restriction of HIV-1 replication in macaques, depending on the species of macaques. The new HIV-1mt clone will be useful for studying molecular mechanisms by which anti-viral host factors regulate HIV-1 replication in macaques.


*Keywords:* HIV-1; Old World monkey; TRIM5α

## 1. Introduction

Human immunodeficiency virus type 1 (HIV-1) productively infects only humans but not Old World monkeys (OWM) such as cynomolgus monkeys (CM) or rhesus monkeys (RM), whereas RM-derived simian immunodeficiency virus (SIVmac) can efficiently replicate in OWM. Because of this species barrier, alternative monkey models using SIVmac or simian/human immunodeficiency viruses (SHIV) have been used for AIDS research [1–4]. However, detailed analyses of molecular mechanisms of the pathogenesis of HIV-1 have been hampered by the lack of appropriate non-human primate models for HIV-1 infection.

The mechanistic basis for the inability of HIV-1 to replicate in OWM cells has remained unclear. Recently, a number of intrinsic anti-HIV-1 cellular factors, including tripartite motif protein 5α (TRIM5α), Cyclophilin A (CypA), apolipoprotein B mRNA-editing catalytic polypeptide (APOBEC3) family and Tetherin were discovered in OWM cells [5,6]. TRIM5α strongly suppresses HIV-1 replication, mainly by affecting the viral disassembly step, resulting in a decrease of reverse transcription products [7,8]. CypA acts as a regulator promoting TRIM5α-mediated restriction of HIV-1 [8]. APOBEC3 is also a major regulator of HIV-1 replication [9,10]. APOBEC3 exerts its inhibitory effect mainly by inducing G to A hypermutation

* Corresponding author. Primate Research Institute, Kyoto University, Inuyama 484-8506, Japan. Tel.: +81 568 63 0440; fax: +81 568 63 0459.
*E-mail address:* akari@pri.kyoto-u.ac.jp (H. Akari).
[1] A.S. and M.N. contributed equally to this work.

1286-4579/$ - see front matter © 2010 Institut Pasteur. Published by Elsevier Masson SAS. All rights reserved.
doi:10.1016/j.micinf.2010.10.001

into the viral genome due to its cytidine deaminase activity, while hypermutation-independent inhibitory activity at the stage of reverse transcription is also evident [11]. Tetherin, also referred to as a BST-2, was identified as an intrinsic anti-viral factor that restricts the egress of HIV-1 by tethering virions to the host cell surface [12,13]. Importantly, HIV-1 can counteract human APOBEC3 activity by utilizing the viral accessory protein Vif, whereas it cannot counteract OWM APOBEC3 [14]. Similarly, HIV-1 counteracts human Tetherin activity by utilizing another viral accessory protein Vpu, whereas HIV-1 does not counteract OWM Tetherin activity [15].

In an attempt to generate a monkey-tropic HIV-1 (HIV-1mt), Kamada et al. constructed an HIV-1 variant carrying minimal SIVmac-derived sequences to overcome the restriction factors [16]. The prototype HIV-1 clone NL-DT5R had a sequence encoding an SIVmac loop between alpha helices 4 and 5 (L4/5) of *capsid* gene (CA) and the entire *vif* gene, which relieved the inhibitory effects on viral replication by restriction factors CypA, TRIM5α and APOBEC3. NL-DT5R was able to replicate in pigtail monkeys (PM) in vivo as well as in vitro, as reported by Igarashi et al. [17]. Although NL-DT5R induced immune responses in infected animals, the virus did not establish persistent infection.

In the present study, we sought to adapt NL-DT5R to CM by performing long-term passage in CM-derived HSC-F cells. We successfully obtained a modified HIV-1mt clone having several mutations. Additionally, we inserted an SIVmac loop between alpha helices 6 and 7 (L6/7) of CA [18]. The resultant clone named MN4-5S was found to replicate efficiently and to induce strong immune responses in infected CM, suggesting the impact of viral adaptation.

## 2. Materials and methods

### 2.1. Plasmid construction

The HIV-1 derivatives were constructed on a background of an infectious molecular clone, NL4-3 [19]. NL-DT5R, a cloned virus containing SIVmac239 L4/5 and the entire *vif* gene, was reported previously by Kamada et al. [16]. In addition, NL-DT562, a virus having an R5-tropic SF162-derived *env* gene on a background of NL-DT5R, was used in this study [20]. After long passage of NL-DT5R and NL-DT562 in cynomolgus T cell line HSC-F [21], several mutations were appeared in both viral genomes, and then all of them were inserted into NL-DT5R by gene-engineering techniques. Consequently, a clone having 14 nucleotide substitutions in its genome was constructed and named MN4-5. Among these substitutions, 7 were non-synonymous mutations. The structure of the clone is shown in Fig. 1. A part of L6/7 of CA (aa residues 120–122; HNP) of MN4-5 was also replaced with the corresponding segment of SIVmac239 CA (aa residues 120–123; RQQN) by means of site-directed mutagenesis as described previously in Ref. [18]. The resultant construct was designated MN4-5S.

### 2.2. Cells and viruses

Human embryonic kidney cell line HEK293T was maintained in DMEM supplemented with 10% fetal bovine serum, 100 units/ml of penicillin and 100 μg/ml of streptomycin (Sigma). Monkey peripheral blood mononuclear cells (PBMCs) were separated with a standard Ficoll density gradient separation method and cultured in R-10 composed of

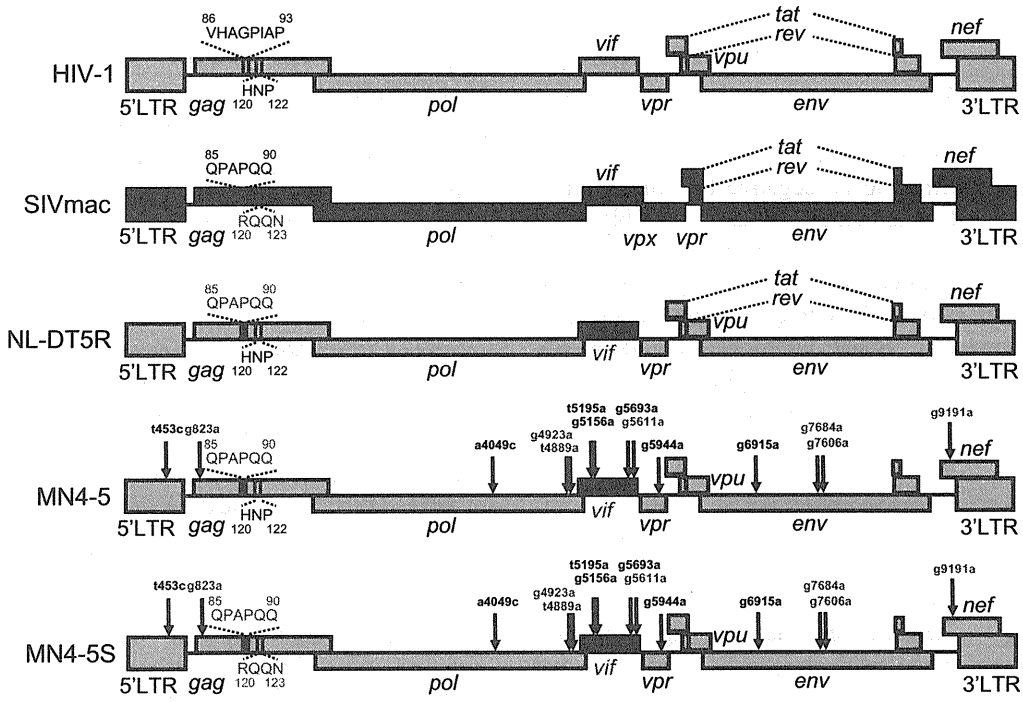


Fig. 1. Structure of HIV-1mt clones used in this study. The positions of nucleotide mutations are indicated by arrows in this figure. Among nucleotide substitutions, the positions of non-synonymous mutations are indicated in red.

RPMI-1640 medium supplemented with 10% fetal bovine serum, 100 units/ml of penicillin and 100 μg/ml of streptomycin (Sigma). The growth kinetics of each HIV-1 clone were examined in activated $CD8^+$ cell-depleted PBMCs. Briefly, separated PBMCs were reacted with a PE-labeled anti-CD8 antibody and then treated with anti-PE magnetic beads. After washing, $CD8^+$ cell-depleted PBMCs were negatively separated by using MACS columns (Miltenyi Biotec). For stimulation, $CD8^+$ cell-depleted PBMCs were first cultured in R-10 containing 1 μg/ml of concanavalin A (Sigma) for 2 days followed by culture in R-10 supplemented with 100 U/ml IL-2 (Shionogi) for more 2 days. The cells were then infected with 100 ng of p24 of HIV-1 and the culture supernatant was collected periodically. HSC-F, a cynomolgus monkey-derived $CD4^+$ T cell line [21], was cultured in R-10.

Virus stocks were prepared as follows: sub-confluent HEK293T cells were transfected with proviral DNA using Lipofectamine2000 reagent according to the manufacturer's instructions. At 42 h after transfection, culture supernatants were centrifuged, filtrated with a 0.45 μm filter, and aliquoted as virus stocks for in vitro experiments. For preparation of viral stocks for in vivo experiments, $CD8^+$ cell-depleted PBMCs were infected with the HEK293T-derived stocks as described above. After washing, the cells were maintained for several days and the culture supernatants were collected and stored as described above.

### 2.3. Reverse transcription (RT) assay

Virion-associated RT activity was measured as described previously in Ref. [22]. HSC-F cells ($1 \times 10^6$) were infected with equal amounts of viruses ($1 \times 10^7$ RT units). Viral growth kinetics was determined by RT production in the culture supernatants.

### 2.4. Animal experiments

Healthy adult cynomolgus monkeys were used in this study. All animals were confirmed to be negative for simian retrovirus and were housed in individual isolators in a biosafety level 3 facility and maintained according to the National Institute of Biomedical Innovation rules and guidelines for experimental animal welfare. Bleeding and viral inoculation were performed under ketamine hydrochloride anesthesia. Viral stocks for inoculation were inoculated into each animal. The profiles of plasma viral RNA loads, circulating $CD4^+$ and $CD8^+$ T lymphocytes were evaluated as described below.

### 2.5. Flow cytometry and immunophenotyping of peripheral blood lymphocytes

Immunophenotyping of freshly isolated PBMCs was performed according to standard procedures using multicolor flow cytometry performed with a FACSCantoII (Becton Dickinson). $CD4^+$ and $CD8^+$ T cells were identified using monoclonal antibodies (mAbs) to CD3 (clone SP34-2, BD Pharmingen), CD4 (clone L200, BD Pharmingen) and CD8 (clone DK25, DAKO). Flow cytometric acquisition and analysis of samples was performed on at least 10,000 events collected by a flow cytometer driven by FACSDiVa software.

### 2.6. Analysis of anti-viral antibody response

Plasma samples from infected animals were first heat-inactivated at 56 °C for 30 min. Then, 100-fold diluted samples were reacted with commercially available anti-HIV-1 antibody detection strips (New LAV Blot I, Bio-Rad) according to the manufacture's instructions.

### 2.7. In vivo depletion of $CD8^+$ lymphocytes

Infected animals received an anti-CD8 mAb (cM-T807) as follows: 10 mg/kg (body weight) inoculation subcutaneously at 42 days post infection (DPI), followed by 5 mg/kg inoculation intravenously at 45, 49, and 52 DPI. The cM-T807 mAb was provided by the NIH Nonhuman Primate Reagent Resource. To repeatedly confirm the depletion of $CD8^+$ cells in the presence of cM-T807, an anti-CD8 mAb (clone DK25, DAKO) was used as reported previously in Ref. [23].

### 2.8. Quantification of viral RNA

Total RNA was collected from monkey plasma using a High Pure Viral RNA Kit (Roche Diagnostics) according to the manufacturer's instructions. Viral RNA was quantified with a quantitative real-time PCR system using TaqMan One-Step RT-PCR Master Mix Reagents (Applied Biosystems). The primers and probe used in this study were as follows: Forward primer: HIVgag683 (+) (5′-CTCTCGACGCAGGACTCGGCTTGCT-3′); Reverse primer: HIVgag803 (−) (5′-GCTCTCGCACCCATCTCTCTCCTTCTAGCC-3′); Probe: HIVgag TaqMan 720R748 (FAM-GCAAGAGGCGAGRGGCGGCGACTGGTGAG-TAMRA). The quantification and data analysis were performed using the iQ5 Real-Time PCR Detection System (Bio-Rad). The detection limit of this assay was 400-copies/ml plasma.

## 3. Results

### 3.1. Growth properties of prototype HIV-1mt clone, NL-DT5R in macaques in vitro and in vivo

We first examined the replication properties of prototype HIV-1mt NL-DT5R in $CD8^+$ cell-depleted PBMCs of CM and RM. NL-DT5R replicated in the cells of CM but not in those of RM (Fig. 2). We next examined the in vivo replication properties of NL-DT5R in CM. Viral stocks for inoculation were prepared with $CD8^+$ cell-depleted CM PBMCs as described above. Then, two monkeys were infected with NL-DT5R intravenously and bled periodically. As shown in Fig. 3A, NL-DT5R established infection as indicated by detectable levels of plasma viremia and an anti-HIV-1 antibody response, although the viral level was marginal (about $1 \times 10^3$ copies/ml) and disappeared at 4 weeks post infection.

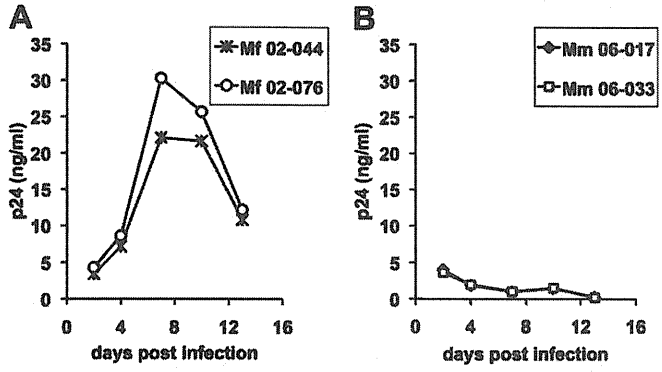


Fig. 2. Growth properties of the NL-DT5R in $CD8^+$ cell-depleted PBMCs from CM (A) and RM (B). The cells were infected with NL-DT5R and the viral replication was monitored by p24 antigen in the culture supernatants using a p24 quantitative ELISA kit. Animal identifications are indicated at the top of each panel.

These results indicated that although CM appeared permissive for NL-DT5R as compared with RM, the mutations introduced in NL-DT5R were not still sufficient to overcome the restriction by host factor(s) of these macaques.

### *3.2. MN4-5S showed improved replication capability in CM $CD8^+$ cell-depleted PBMCs*

In order to improve the replication capability of HIV-1mt in CM, we conducted long-term passage of NL-DT5R in HSC-F cells. Additionally, NL-DT562, having an R5-tropic *env* gene on a background of NL-DT5R, was also passaged long-term in HSC-F cells. We found that the passaging improved the growth of the viruses (data not shown), and then viral clones were obtained after the long-term passaging and sequenced. Ten nucleotide substitutions were identified in the NL-DT5R-derived clone and 4 nucleotide substitutions (except for the *env* gene) in the NL-DT562-derived clone. These 14 nucleotide substitutions (7 of which were non-synonymous mutations) were assembled and introduced into NL-DT5R. The resultant clone was named MN4-5, and its structure is shown in Fig. 1. We previously found that insertion of an SIVmac loop between alpha helices 6 and 7 (L6/7) of CA into the corresponding region in HIV-1 significantly enhanced the viral replication in HSC-F cells and PBMCs of CM by relieving the inhibitory effect of TRIM5α [18]. We therefore inserted an SIVmac-derived L6/7 sequence into MN4-5. The resultant clone was named MN4-5S (Fig. 1). In order to examine the impact of these modifications on the viral replication, we analyzed the replication properties of this "adapted" virus in HSC-F cells and $CD8^+$ cell-depleted PBMCs of CM. MN4-5 showed higher replication as compared with NL-DT5R in both types of cells (Figs. 4 and 5). Moreover, MN4-5S showed enhanced growth capability in the cells as compared with the parental clones, NL-DT5R and MN4-5 (Figs. 4 and 5).

Notably, MN4-5S did not show any replication in RM cells (data not shown), indicating that the combination of the mutations introduced in NL-DT5R may be effective for escape from the restriction in CM cells but not in RM cells.

### *3.3. MN4-5S induced greater viremia in CM as compared with parental clone, NL-DT5R*

Since MN4-5S showed enhanced ability to replicate in CM cells, we next examined the viral replication in vivo. The stock of MN4-5S virus was inoculated into 3 CM. MN4-5S induced 10-fold higher viremia in infected animals at 2–3 weeks after infection (Fig. 6A), as compared with that induced by NL-DT5R (see Fig. 3). This result was consistent with the in vitro result (Fig. 5) and demonstrated that the mutations inserted into NL-DT5R contributed to enhancement of viral replication in vivo. In addition, at the acute phase of infection a slight decrease of $CD4^+$ T cells was observed (Fig. 6B). The viremia became undetectable at 6 weeks after infection.

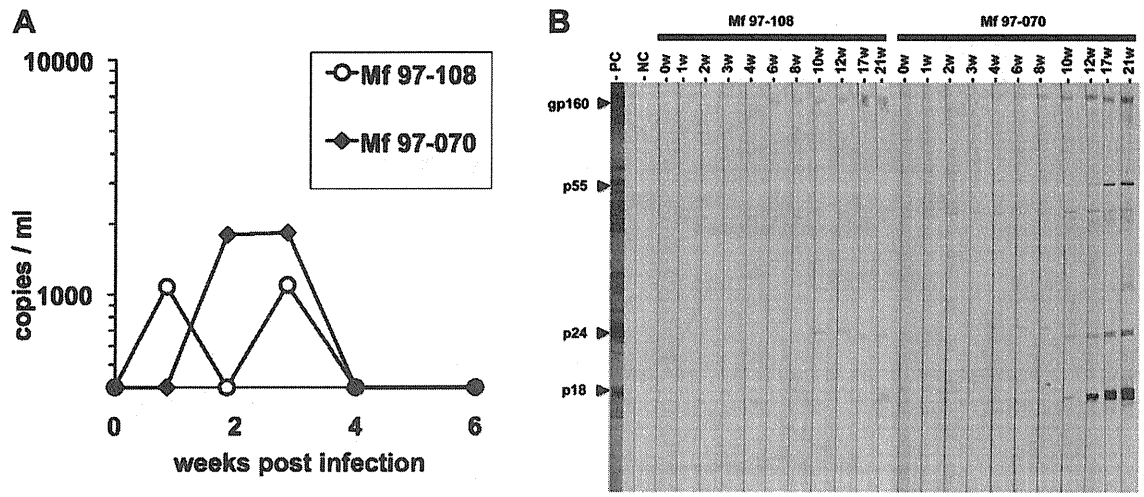


Fig. 3. Profiles of plasma viral RNA loads (A) and anti-HIV-1 antibody responses (B) in CM infected with NL-DT5R. Mf97-108 (open circles) and Mf97-070 (closed diamonds) were used in this study. Viral stocks for inoculation were prepared in $CD8^+$ cell-depleted PBMCs, and then 6.1 ng p24 of HIV-1 were inoculated into each animal. Commercially available diagnostic HIV-1 Western blotting strips were reacted with 100-fold diluted monkey plasma. Plasma from HIV-1-infected or uninfected individuals was used as a positive or a negative control, respectively.

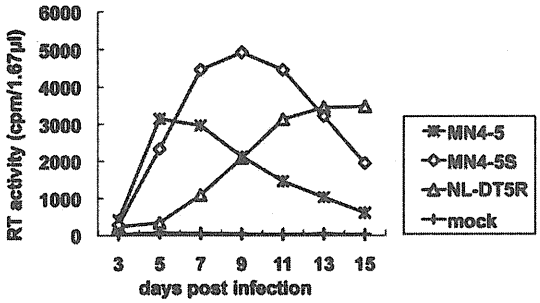


Fig. 4. Growth properties of HIV-1mt in HSC-F cells. The cells were infected with a series of HIV-1mt derivatives. The viral replication was monitored by RT activity in the culture supernatants.

Thereafter, antibody response against MN4-5S was observed in infected animals (Fig. 6C). As indicated by comparison with the lane of the positive control as a standard, the degree of antibody response seemed to be stronger than that against NL-DT5R (see Figs. 3B and 6C). Next we attempted to clarify the role of $CD8^+$ lymphocytes in the disappearance of viremia. We conducted in vivo depletion of $CD8^+$ cells by using a method reported previously [23]. We found that the reappearance of viremia was observed in all monkeys tested in parallel with the decline of $CD8^+$ T cells after the anti-CD8 mAb administration (Fig. 6A and D). This result indicated that $CD8^+$ T cells had a critical role in the control of HIV-1mt replication and suggested that the virus was able to infect latently in vivo.

## 4. Discussion

In the present study, we found that a modified HIV-1mt, MN4-5S, acquired greater ability to replicate in CM than NL-DT5R, and that both the SIVmac-derived L6/7 (HNP120-122 > RQQN120-123 of CA) and a series of substitutions identified by long-term passage of NL-DT5R in HSC-F cells contributed to this ability (Fig. 1). We recently showed that the substitution of L6/7 relieved the inhibitory effect of TRIM5α [18]. Additionally, our preliminary data suggest that non-synonymous mutations in the *integrase* and *env* genes are likely to be critical for the improved activity (Nomaguchi et al., manuscript in preparation). It is possible that these adaptive mutations may optimize the interaction between host and viral proteins.

It seemed that the growth kinetics of NL-DT5R in PM were comparable with those of MN4-5S in CM, which had peak levels in acute viremia of approximately $10^4$ copies/ml [17]. It is therefore likely that PM may exhibit better susceptibility to HIV-1mt than CM. It is possible that the greater susceptibility of PM to HIV-1mt replication could be due to the genotype of TRIM5, because PM usually expresses a chimera between TRIM5α and CypA, so-called TRIM-Cyp, whose anti-HIV-1 activity is defective [24].

One unexpected finding in this study was that MN4-5S was unable to replicate in PBMCs of RM (data not shown), which was in contrast with the greater susceptibility of RM to SIV-mac infection. Our results suggested that RM was most resistant to HIV-1mt replication among the three macaque species. Since our HIV-1mt clones (NL-DT5R and MN4-5) were established on the basis of information obtained from serial passages of the viruses in CM-derived cells, it may be reasonable to consider that these viruses were consequently optimized to CM. Alternatively, it is also possible that anti-HIV-1 activities such as TRIM5α and APOBEC3 of RM could be greater than those of other macaques. Further studies are in progress to address these questions.

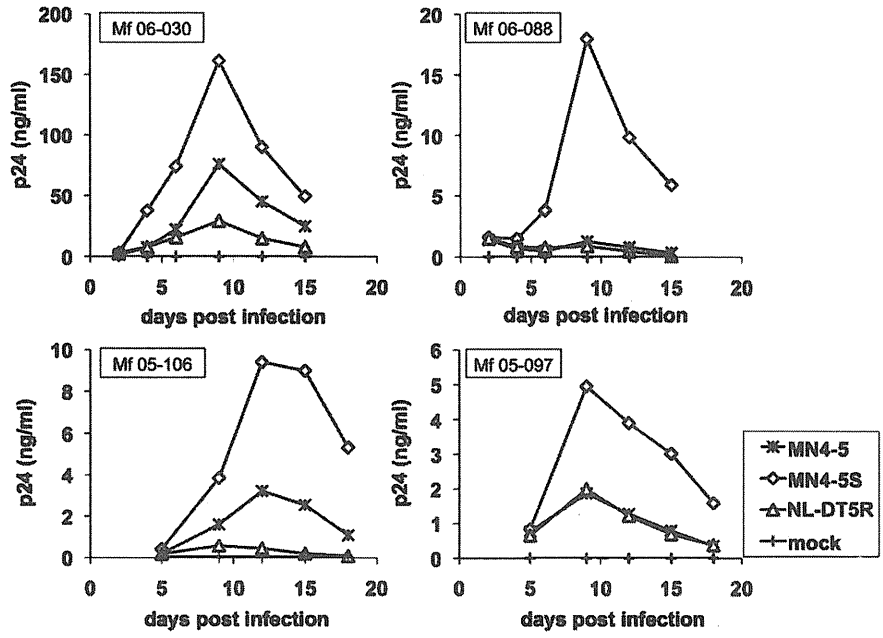


Fig. 5. Growth properties of HIV-1mt in $CD8^+$ cell-depleted PBMCs from four CM. The cells were infected with a series of HIV-1mt derivatives. The viral replication was monitored by p24 antigen in the culture supernatants using a p24 quantitative ELISA kit. Animal identifications are indicated at the top of each panel.

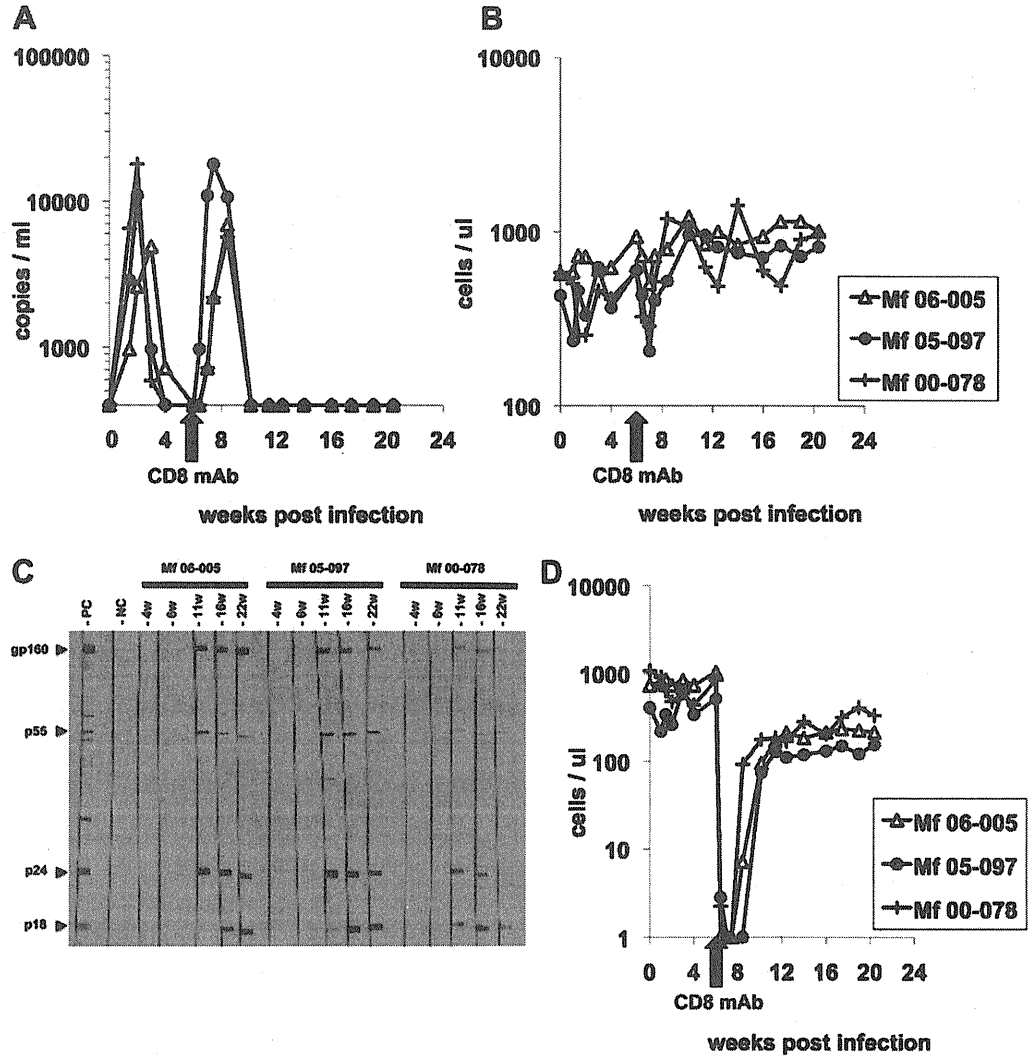


Fig. 6. Profiles of plasma viral RNA loads (A), circulating $CD4^+$ T lymphocytes (B), anti-HIV-1 antibody responses (C) and circulating $CD8^+$ T lymphocytes (D) in CM infected with HIV-1 derivatives. Viral stocks for inoculation were prepared in $CD8^+$ cell-depleted PBMCs and then 10 ng of p24 of HIV-1 were inoculated into each animal. Commercially available diagnostic HIV-1 Western blotting strips were reacted with 100-fold diluted plasma of each monkey. Plasma from HIV-1 infected or uninfected individuals was used as a positive or negative control, respectively. The black arrow indicates the day of anti-CD8 mAb (cM-T807) inoculation.

We demonstrated that the reappearance of viremia was observed in all monkeys tested in parallel with decline of $CD8^+$ T cells after anti-CD8 mAb administration (Fig. 6A and D). This result indicated that HIV-1-specific $CD8^+$ T cells had a critical role in the control of HIV-1mt replication and suggested that the virus may be able to infect latently in vivo. In order to establish a set point viremia and persistent infection, further modifications of HIV-1mt may be required to enable potent escape from the anti-viral immune response.

Further mechanistic characterization of anti-HIV-1 restriction factors will help in the construction of highly replicative and pathogenic HIV-1mt clones. As in the case of SHIV, in vivo passage of the virus could be a conventional and straightforward procedure for achieving such purposes [4]. However, the results of our study demonstrate that selective modification of HIV-1mt based on available knowledge regarding the molecular machineries is an alternative and powerful way. We are now in the process of developing the next generation of HIV-1mt that will acquire growth ability and pathogenicity in macaques as well as in humans.

## Acknowledgements

The authors wish to thank T. Kurosawa, M. Fujita and M. Yasue for their helpful assistance. The authors also thank F. Ono, Y. Katakai, K. Komatsuzaki, A. Hiyaoka, K. Ohto, H. Ohto, and Y. Emoto for their support in animal experiments. We also thank M. Kaizu for his technical support. The anti-CD8 antibody used in the present study was provided by the NIH Nonhuman Primate Reagent Resource (R24 RR016001, N01 AI040101). This work was supported by grants from the Japan Health Sciences Foundation and the Ministry of Health, Labor, and Welfare in Japan and by Global COE Program A06 of Kyoto University.

## References


[1] N.L. Letvin, M.D. Daniel, P.K. Sehgal, R.C. Desrosiers, R.D. Hunt, L.M. Waldron, J.J. MacKey, D.K. Schmidt, L.V. Chalifoux, N.W. King, Induction of AIDS-like disease in macaque monkeys with T-cell tropic retrovirus STLV-III, Science 230 (1985) 71–73.

[2] H. Kestler, T. Kodama, D. Ringler, M. Marthas, N. Pedersen, A. Lackner, D. Regier, P. Sehgal, M. Daniel, N. King, et al., Induction of AIDS in rhesus monkeys by molecularly cloned simian immunodeficiency virus, Science 248 (1990) 1109–1112.

[3] R. Shibata, M. Kawamura, H. Sakai, M. Hayami, A. Ishimoto, A. Adachi, Generation of a chimeric human and simian immunodeficiency virus infectious to monkey peripheral blood mononuclear cells, J. Virol. 65 (1991) 3514–3520.

[4] K.A. Reimann, J.T. Li, R. Veazey, M. Halloran, I.W. Park, G.B. Karlsson, J. Sodroski, N.L. Letvin, A chimeric simian/human immunodeficiency virus expressing a primary patient human immunodeficiency virus type 1 isolate env causes an AIDS-like disease after in vivo passage in rhesus monkeys, J. Virol. 70 (1996) 6922–6928.

[5] M. Nomaguchi, N. Doi, K. Kamada, A. Adachi, Species barrier of HIV-1 and its jumping by virus engineering, Rev. Med. Virol. 18 (2008) 261–275.

[6] D. Sauter, A. Specht, F. Kirchhoff, Tetherin: holding on and letting go, Cell 141 (2010) 392–398.

[7] M. Stremlau, C.M. Owens, M.J. Perron, M. Kiessling, P. Autissier, J. Sodroski, The cytoplasmic body component TRIM5alpha restricts HIV-1 infection in Old World monkeys, Nature 427 (2004) 848–853.

[8] E.E. Nakayama, T. Shioda, Anti-retroviral activity of TRIM5 alpha, Rev. Med. Virol. 20 (2010) 77–92.

[9] A.M. Sheehy, N.C. Gaddis, J.D. Choi, M.H. Malim, Isolation of a human gene that inhibits HIV-1 infection and is suppressed by the viral Vif protein, Nature 418 (2002) 646–650.

[10] S. Henriet, G. Mercenne, S. Bernacchi, J.C. Paillart, R. Marquet, Tumultuous relationship between the human immunodeficiency virus type 1 viral infectivity factor (Vif) and the human APOBEC-3G and APOBEC-3F restriction factors, Microbiol. Mol. Biol. Rev. 73 (2009) 211–232.

[11] M.H. Malim, APOBEC proteins and intrinsic resistance to HIV-1 infection, Philos. Trans. R Soc. Lond B. Biol. Sci. 364 (2009) 675–687.

[12] S.J. Neil, T. Zang, P.D. Bieniasz, Tetherin inhibits retrovirus release and is antagonized by HIV-1 Vpu, Nature 451 (2008) 425–430.

[13] J.L. Douglas, J.K. Gustin, K. Viswanathan, M. Mansouri, A.V. Moses, K. Fruh, The great escape: viral strategies to counter BST-2/tetherin, PLoS Pathog. 6 (2010) e1000913.

[14] R. Mariani, D. Chen, B. Schrofelbauer, F. Navarro, R. Konig, B. Bollman, C. Munk, H. Nymark-McMahon, N.R. Landau, Species-specific exclusion of APOBEC3G from HIV-1 virions by Vif, Cell 114 (2003) 21–31.

[15] B. Jia, R. Serra-Moreno, W. Neidermyer, A. Rahmberg, J. Mackey, I.B. Fofana, W.E. Johnson, S. Westmoreland, D.T. Evans, Species-specific activity of SIV Nef and HIV-1 Vpu in overcoming restriction by tetherin/BST2, PLoS Pathog. 5 (2009) e1000429.

[16] K. Kamada, T. Igarashi, M.A. Martin, B. Khamsri, K. Hatcho, T. Yamashita, M. Fujita, T. Uchiyama, A. Adachi, Generation of HIV-1 derivatives that productively infect macaque monkey lymphoid cells, Proc Natl Acad Sci U S A 103 (2006) 16959–16964.

[17] T. Igarashi, R. Iyengar, R.A. Byrum, A. Buckler-White, R.L. Dewar, C. E. Buckler, H.C. Lane, K. Kamada, A. Adachi, M.A. Martin, Human immunodeficiency virus type 1 derivative with 7% simian immunodeficiency virus genetic content is able to establish infections in pig-tailed macaques, J. Virol. 81 (2007) 11549–11552.

[18] A. Kuroishi, A. Saito, Y. Shingai, T. Shioda, M. Nomaguchi, A. Adachi, H. Akari, E.E. Nakayama, Modification of a loop sequence between alpha-helices 6 and 7 of virus capsid (CA) protein in a human immunodeficiency virus type 1 (HIV-1) derivative that has simian immunodeficiency virus (SIVmac239) vif and CA alpha-helices 4 and 5 loop improves replication in cynomolgus monkey cells, Retrovirology 6 (2009) 70.

[19] A. Adachi, H.E. Gendelman, S. Koenig, T. Folks, R. Willey, A. Rabson, M.A. Martin, Production of acquired immunodeficiency syndrome-associated retrovirus in human and nonhuman cells transfected with an infectious molecular clone, J. Virol. 59 (1986) 284–291.

[20] T. Yamashita, N. Doi, A. Adachi, M. Nomaguchi, Growth ability in simian cells of monkey cell-tropic HIV-1 is greatly affected by downstream region of the vif gene, J. Med. Invest. 55 (2008) 236–240.

[21] H. Akari, K.H. Nam, K. Mori, I. Otani, H. Shibata, A. Adachi, K. Terao, Y. Yoshikawa, Effects of SIVmac infection on peripheral blood CD4+CD8+ T lymphocytes in cynomolgus macaques, Clin. Immunol. 91 (1999) 321–329.

[22] R.L. Willey, D.H. Smith, L.A. Lasky, T.S. Theodore, P.L. Earl, B. Moss, D.J. Capon, M.A. Martin, In vitro mutagenesis identifies a region within the envelope gene of the human immunodeficiency virus that is critical for infectivity, J. Virol. 62 (1988) 139–147.

[23] J.E. Schmitz, M.A. Simon, M.J. Kuroda, M.A. Lifton, M.W. Ollert, C.W. Vogel, P. Racz, K. Tenner-Racz, B.J. Scallon, M. Dalesandro, J. Ghrayeb, E.P. Rieber, V.G. Sasseville, K.A. Reimann, A nonhuman primate model for the selective elimination of CD8+ lymphocytes using a mouse-human chimeric monoclonal antibody, Am. J. Pathol. 154 (1999) 1923–1932.

[24] C.A. Virgen, Z. Kratovac, P.D. Bieniasz, T. Hatziioannou, Independent genesis of chimeric TRIM5-cyclophilin proteins in two primate species, Proc. Natl. Acad. Sci. U S A 105 (2008) 3563–3568.

Biochemical and Biophysical Research Communications 408 (2011) 615–619

Contents lists available at ScienceDirect

Biochemical and Biophysical Research Communications

journal homepage: www.elsevier.com/locate/ybbrc

# Dominant induction of vaccine antigen-specific cytotoxic T lymphocyte responses after simian immunodeficiency virus challenge

Yusuke Takahara [a,b], Saori Matsuoka [b], Tetsuya Kuwano [a], Tetsuo Tsukamoto [a], Hiroyuki Yamamoto [b], Hiroshi Ishii [a,b], Tadashi Nakasone [b], Akiko Takeda [b], Makoto Inoue [c], Akihiro Iida [c], Hiroto Hara [c], Tsugumine Shu [c], Mamoru Hasegawa [c], Hiromi Sakawaki [d], Mariko Horiike [d], Tomoyuki Miura [d], Tatsuhiko Igarashi [d], Taeko K. Naruse [e], Akinori Kimura [e], Tetsuro Matano [a,b,*]

[a] Division for AIDS Vaccine Development, The Institute of Medical Science, The University of Tokyo, 4-6-1 Shirokanedai, Minato-ku, Tokyo 108-8639, Japan
[b] AIDS Research Center, National Institute of Infectious Diseases, 1-23-1 Toyama, Shinjuku-ku, Tokyo 162-8640, Japan
[c] DNAVEC Corporation, 6 Ohkubo, Tsukuba, Ibaraki 300-2611, Japan
[d] Institute for Virus Research, Kyoto University, 53 Kawahara-cho, Shogoin, Sakyo-ku, Kyoto 606-8507, Japan
[e] Department of Molecular Pathogenesis, Medical Research Institute, Tokyo Medical and Dental University, 2-3-10 Kandasurugadai, Chiyoda-ku, Tokyo 101-0062, Japan

ARTICLE INFO

*Article history:*
Received 12 April 2011
Available online 21 April 2011

*Keywords:*
AIDS vaccine
HIV
SIV
CTL
Immunodominance

ABSTRACT

Cytotoxic T lymphocyte (CTL) responses are crucial for the control of human and simian immunodeficiency virus (HIV and SIV) replication. A promising AIDS vaccine strategy is to induce CTL memory resulting in more effective CTL responses post-viral exposure compared to those in natural HIV infections. We previously developed a CTL-inducing vaccine and showed SIV control in some vaccinated rhesus macaques. These vaccine-based SIV controllers elicited vaccine antigen-specific CTL responses dominantly in the acute phase post-challenge. Here, we examined CTL responses post-challenge in those vaccinated animals that failed to control SIV replication. Unvaccinated rhesus macaques possessing the major histocompatibility complex class I haplotype *90-088-Ij* dominantly elicited SIV non-Gag antigen-specific CTL responses after SIV challenge, while those induced with Gag-specific CTL memory by prophylactic vaccination failed to control SIV replication with dominant Gag-specific CTL responses in the acute phase, indicating dominant induction of vaccine antigen-specific CTL responses post-challenge even in non-controllers. Further analysis suggested that prophylactic vaccination results in dominant induction of vaccine antigen-specific CTL responses post-viral exposure but delays SIV non-vaccine antigen-specific CTL responses. These results imply a significant influence of prophylactic vaccination on CTL immunodominance post-viral exposure, providing insights into antigen design in development of a CTL-inducing AIDS vaccine.



## 1. Introduction

In human and simian immunodeficiency virus (HIV and SIV) infections, cytotoxic T lymphocyte (CTL) responses exert strong suppressive pressure on viral replication but fail to control viremia leading to AIDS progression [1–5]. A promising AIDS vaccine strategy is to induce CTL memory resulting in more effective CTL responses post-viral exposure compared to those in natural HIV infections. It is important to determine how prophylactic CTL memory induction affects CTL responses in the acute phase post-viral exposure.

We previously developed a prophylactic AIDS vaccine (referred to as DNA/SeV-Gag vaccine) consisting of DNA priming followed by boosting with a recombinant Sendai virus (SeV) vector expressing SIVmac239 Gag [6]. Evaluation of this vaccine's efficacy against a SIVmac239 challenge in Burmese rhesus macaques showed that some vaccinees contained SIV replication [7]. In particular, vaccination consistently resulted in SIV control in those animals possessing the major histocompatibility complex class I (MHC-I) haplotype *90-120-Ia* [8]; $Gag_{206-216}$ (IINEEAADWDL) and $Gag_{241-249}$ (SSVDEQIQW) epitope-specific CTL responses were shown to be responsible for this vaccine-based SIV control [9]. Furthermore, in a SIVmac239 challenge experiment of *90-120-Ia*-positive macaques that received a prophylactic DNA/SeV vaccine expressing the $Gag_{241-249}$ epitope fused with enhanced green fluorescent protein (EGFP), all the vaccinees controlled SIV replication [10]. This single epitope vaccination resulted in dominant $Gag_{241-249}$-specific CTL responses with delayed $Gag_{206-216}$-specific CTL induction after SIV challenge, whereas $Gag_{206-216}$-specific and

* Corresponding author at: AIDS Research Center, National Institute of Infectious Diseases, 1-23-1 Toyama, Shinjuku-ku, Tokyo 162-8640, Japan. Fax: +81 3 5285 1165.
*E-mail address:* tmatano@nih.go.jp (T. Matano).

0006-291X/$ - see front matter © 2011 Elsevier Inc. All rights reserved.
doi:10.1016/j.bbrc.2011.04.071

$Gag_{241-249}$-specific CTL responses were detected equivalently in unvaccinated *90-120-Ia*-positive animals.

These previous results in vaccine-based SIV controllers indicate dominant induction of vaccine antigen-specific CTL responses post-challenge, implying that prophylactic vaccination inducing vaccine antigen-specific CTL memory may delay CTL responses specific for viral antigens other than vaccine antigens (referred to as non-vaccine antigens) post-viral exposure. In these SIV controllers, the reduction of viral loads could be involved in delay of SIV non-vaccine antigen-specific CTL responses. Then, in the present study, we examined the influence of prophylactic vaccination on immunodominance post-challenge in those vaccinees that failed to control SIV replication. Our results showed dominant induction of vaccine antigen-specific CTL responses post-challenge even in these SIV non-controllers.

## 2. Materials and methods

### 2.1. Animal experiments

The first set of experiment used samples in our previous experiments of six Burmese rhesus macaques (Macaca mulatta) possessing the MHC-I haplotype *90-088-Ij* (macaques R02-004, R02-001, and R03-015, previously reported [7,11]; R04-014, R06-022, and R04-011, unpublished). Three of them, R02-001, R04-011, and R03-015, received a prophylactic DNA/SeV-Gag vaccine [7]. The DNA used for the vaccination, CMV-SHIVdEN, was constructed from *env*-deleted and *nef*-deleted simian–human immunodeficiency virus $SHIV_{MD14YE}$ [12] molecular clone DNA (SIVGP1) and has the genes encoding SIVmac239 Gag, Pol, Vif, and Vpx, SIVmac239-HIV chimeric Vpr, and HIV Tat and Rev. At the DNA vaccination, animals received 5 mg of CMV-SHIVdEN DNA intramuscularly. Six weeks after the DNA prime, animals received a single boost intranasally with $6 \times 10^9$ cell infectious units (CIUs) of F-deleted replication-defective SeV-Gag [13,14]. All six *90-088-Ij*-positive animals including three unvaccinated and three vaccinated were challenged intravenously with 1000 50% tissue culture infective doses (TCID50) of SIVmac239 [15] approximately 3 months after the boost. At week 1 after SIV challenge, macaque R03-015 was inoculated with nonspecific immunoglobulin G as previously described [11].

In the second set of experiment, unvaccinated (R06-001) and vaccinated (R05-028) rhesus macaques possessing the MHC-I haplotype *90-120-Ib* were challenged intravenously with 1000 TCID50 of SIVmac239. The latter R05-028 were immunized intranasally with F-deleted SeV-Gag approximately 3 months before the challenge.

In the third, three rhesus macaques received FMSIV plus mCAT1-expressing DNA vaccination three times with intervals of 4 weeks. The FMSIV DNA was constructed by replacing *nef*-deleted $SHIV_{MD14YE}$ with Friend murine leukemia virus (FMLV) *env*, carrying the same SIVmac239-derived antigen-coding regions with SIVGP1, as described before [16]. Vaccination of macaques with FMSIV and a DNA expressing the FMLV receptor (mCAT1) [17] three times with intervals of a week was previously shown to induce mCAT1-dependent confined FMSIV replication resulting in efficient CTL induction while vaccination three times with intervals of 4 weeks in the present study resulted in marginal levels of responses (data not shown). These three DNA-vaccinated animals were challenged intravenously with 1000 TCID50 of SIVmac239 approximately 2 months after the last vaccination.

Some animal experiments were conducted in the Tsukuba Primate Research Center, National Institute of Biomedical Innovation, with the help of the Corporation for Production and Research of Laboratory Primates, in accordance with the guidelines for animal experiments at the National Institute of Infectious Diseases, and others were in Institute for Virus Research, Kyoto University in accordance with the institutional regulations.

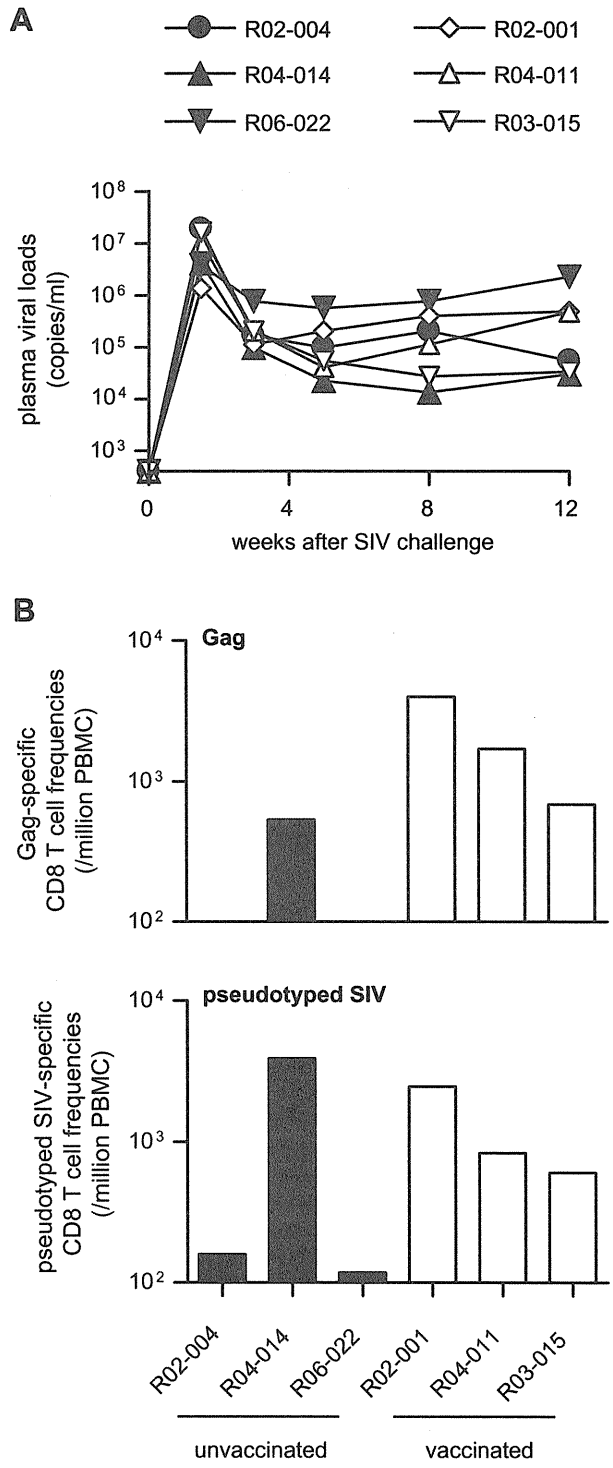


**Fig. 1.** CTL responses after SIVmac239 challenge in *90-088-Ij*-positive macaques. (A) Plasma viral loads after SIV challenge in unvaccinated (R02-004, R04-014, and R06-022) and DNA/SeV-Gag vaccinated animals (R02-001, R04-011, and R03-015). The viral loads (SIV gag RNA copies/ml) were determined as described previously [7]. (B) Vaccine antigen Gag-specific (upper panel) and pseudotyped SIV-specific $CD8^+$ T cell frequencies (lower panel) at week 2 after SIV challenge.

### 2.2. Analysis of virus-specific CTL responses

We measured virus-specific $CD8^+$ T-cell levels by flow cytometric analysis of gamma interferon (IFN-γ) induction after specific

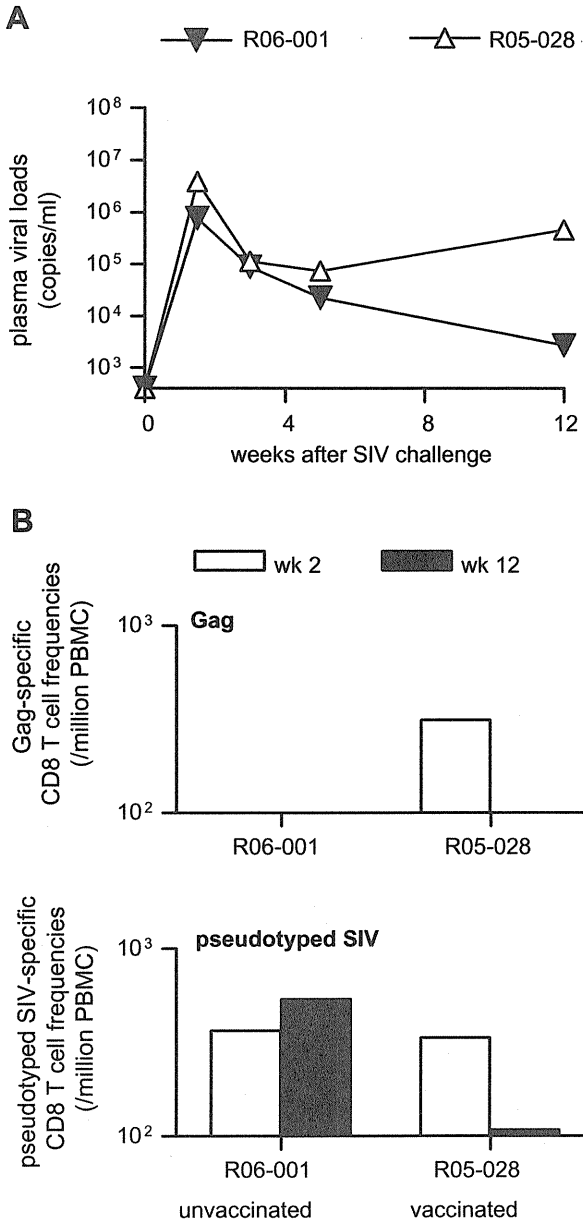


**Fig. 2.** CTL responses after SIVmac239 challenge in *90–120-Ib*-positive macaques. (A) Plasma viral loads after SIV challenge in unvaccinated R06–001 and SeV-Gag-vaccinated macaque R05-028. (B) Vaccine antigen Gag-specific (upper panel) and pseudotyped SIV-specific $CD8^+$ T cell frequencies (lower panel) at weeks 2 (white bars) and 12 (black bars) after SIV challenge.

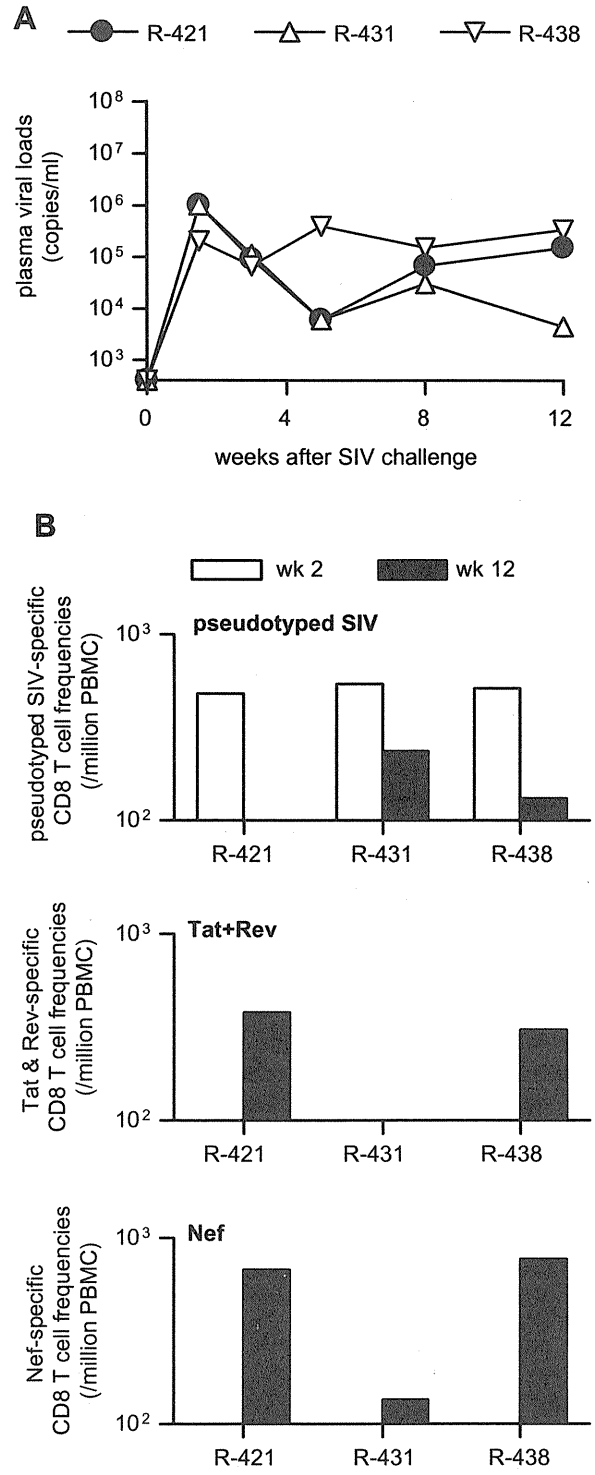


**Fig. 3.** CTL responses after SIVmac239 challenge in DNA-vaccinated macaques. The DNA used for the vaccination has the SIVmac239-derived region encoding Gag, Pol, Vif, and Vpx and is expected to induce pseudotyped SIV-specific CTL responses. (A) Plasma viral loads after SIV challenge in DNA vaccinated macaques R-421, R-431, and R-438. (B) Vaccine antigen (pseudotyped SIV)-specific (top panel), Tat-plus-Rev-specific (middle panel), and Nef-specific $CD8^+$ T cell frequencies (bottom panel) at weeks 2 (white bars) and 12 (black bars) after SIV challenge. In macaque R-438, CTL responses at week 5 instead of week 12 are shown.

stimulation as described previously [18,19]. Peripheral blood mononuclear cells (PBMCs) were cocultured with autologous herpesvirus papio-immortalized B-lymphoblastoid cell lines (B-LCLs) infected with a vaccinia virus vector expressing SIVmac239 Gag for Gag-specific stimulation or a vesicular stomatitis virus G protein (VSV-G)-pseudotyped SIV for pseudotyped SIV-specific stimulation. The pseudotyped SIV was obtained by cotransfection of COS-1 cells with a VSV-G-expression plasmid and SIVGP1 DNA. Alternatively, PBMCs were cocultured with B-LCLs pulsed with peptide pools using panels of overlapping peptides spanning the entire SIVmac239 Tat, Rev, and Nef amino acid sequences. Intracellular IFN-γ staining was performed with a CytofixCytoperm kit (Becton Dickinson, Tokyo, Japan) and fluorescein isothiocyanate-conjugated anti-human CD4, peridinin chlorophyll protein-conjugated anti-human CD8, allophycocyanin-conjugated anti-human CD3, and phycoerythrin-conjugated anti-human IFN-γ monoclonal antibodies (Becton Dickinson). Specific $CD8^+$ T-cell levels were calculated by subtracting nonspecific IFN-$\gamma^+$ $CD8^+$ T-cell frequencies from those after Gag-specific, pseudotyped

| | vaccine antigen | | | | | non-vaccine antigen | | | | | | | | | | |
|---|---|---|---|---|---|---|---|---|---|---|---|---|---|---|---|---|
| | Gag | | | | Vif | Vpr | Tat | | | | | Rev | | Nef | | |
| | 165 | 333 | 375 | 376 | 143 | 73 | 23 | 115 | 120 | 122 | 125 | 45 | 50 | 63 | 100 | 124 |
| wk 5 | | | | | | | | | | | | | | | | |
| R- 421 | | | | | ++ | | | | | | | | | | | |
| R- 431 | | | | | + | | | | | | | | | | | |
| R- 438 | ++ | | + | | | | | | | ++ | | | | | | |
| wk 12 | | | | | | | | | | | | | | | | |
| R- 421 | | ++ | | | ++ | | | | + | | + | + | + | | | ++ |
| R- 431 | | | | | + | | + | | | ++ | | | | | | |
| R- 438 | ++ | | | ++ | | + | | ++ | | | | | | ++ | ++ | |

**Fig. 4.** Viral mutations in DNA-vaccinated macaques. Plasma viral genome sequencing was performed as described previously [18] to determine mutations resulting in amino acid substitutions in SIV Gag, Pol, Vif, Vpx, Vpr, Tat, Rev, and Nef antigens (except for Env) at weeks 5 and 12 in DNA-vaccinated macaques. The amino acid positions showing mutant sequences dominantly (++) or equivalently with wild type (+) are shown. While we found a mutation leading to a lysine-to-arginine alteration at the 40th amino acid in Rev in all animals, this mutation is not shown because the wild-type sequence at this position in the SIVmac239 molecular clone is considered to be a suboptimal nucleotide that frequently reverts to an alternative sequence in vivo [18,23].

SIV-specific, or peptide-specific stimulation. Specific $CD8^+$ T-cell levels lower than 100 per million PBMCs were considered negative.

## 3. Results and discussion

In our previous SIVmac239 challenge experiments, the prophylactic DNA/SeV-Gag vaccination did not result in viral control in rhesus macaques possessing the MHC-I haplotype *90-088-Ij*. These vaccinated animals showed similar levels of plasma viral loads as those in unvaccinated *90-088-Ij*-positive animals after SIV challenge (Fig. 1A). Analysis of virus-specific $CD8^+$ T-cell responses using PBMCs at week 2 after challenge showed equivalent Gag-specific and pseudotyped SIV-specific (Gag-, Pol-, Vif-, and Vpx-specific) CTL responses in all three vaccinees (Fig. 1B). Pseudotyped SIV-specific CTL responses were also detected in all three unvaccinated animals, but Gag-specific CTL responses were undetectable in two out of the three; even the Gag-specific CTL responses detected in macaque R04-014 were much lower than pseudotyped SIV-specific CTL responses, indicating dominant induction of CTL responses specific for SIV antigens other than Gag (Fig. 1B). Thus, in the acute phase of SIV infection, SIV non-Gag antigen-specific CTL responses were dominantly induced in unvaccinated *90-088-Ij*-positive macaques, whereas vaccine antigen (Gag)-specific CTL responses were dominant in *90-088-Ij*-positive vaccinees.

We then analyzed another vaccinees that failed to control a SIVmac239 challenge; these macaques were vaccinated with SeV-Gag alone or DNA alone. First, we compared post-challenge CTL responses in unvaccinated and SeV-Gag-vaccinated macaques possessing the MHC-I haplotype *90-120-Ib*. Both macaques failed to control SIV replication after challenge (Fig. 2A). In the unvaccinated animal R06-001, Gag-specific CTL responses were undetectable but pseudotyped SIV-specific CTL responses were induced efficiently at weeks 2 and 12 (Fig. 2B). In contrast, Gag-specific CTL responses were induced efficiently at week 2 in the SeV-Gag-vaccinated animal R05-028 (Fig. 2B). At week 12, Gag-specific CTL responses became undetectable while pseudotyped SIV-specific CTL responses were still detectable in this animal. These results indicate that, in the acute phase after SIVmac239 challenge, the unvaccinated *90-120-Ib*-positive macaque dominantly elicited SIV non-Gag antigen-specific CTL responses whereas the SeV-Gag-vaccinated *90-120-Ib*-positive macaque dominantly induced vaccine antigen (Gag)-specific CTL responses.

Next, we analyzed post-challenge CTL responses in three DNA-vaccinated macaques. These animals failed to control SIVmac239 replication after challenge (Fig. 3A). The DNA used for the vaccination and the pseudotyped SIV genome both have the same SIVmac239-derived region encoding Gag, Pol, Vif, and Vpx, thus expected to induce pseudotyped SIV-specific CTL responses. Pseudotyped SIV-specific CTL responses, namely vaccine antigen-specific CTL responses, were induced efficiently at week 2 but diminished after that in all three animals (Fig. 3B). In contrast, Tat/Rev- and Nef-specific CTL responses were undetectable at week 2 but induced later (Fig. 3B). Again, vaccine antigen-specific CTL responses were dominantly induced in the acute phase after SIV challenge and non-vaccine antigen-specific CTL responses were elicited later.

All three animals showed viral genome mutations leading to amino acid substitutions in Gag or Vif at week 5 (Fig. 4). Further analysis indicated that viral mutations in vaccine antigen-coding regions appeared earlier than those in other regions. These results may reflect selective pressure on SIV by vaccine antigen-specific CTL responses dominantly induced in the acute phase, although it remains undetermined whether these mutations are CTL escape ones. Disappearance of vaccine antigen-specific CTL responses at week 12 may be explained by rapid selection of CTL escape mutations in vaccine antigen-coding regions. However, analysis using peptides found Gag-specific CTL responses in macaques R-421 and R-431 that had no gag mutations at week 5 (data not shown), suggesting involvement of immunodominance [20] in the disappearance of vaccine antigen-specific CTL responses at week 12.

In summary, the present study indicates that vaccine antigen-specific CTL responses are induced dominantly in the acute phase after viral exposure, with delayed induction of CTL responses specific for SIV non-vaccine antigens (SIV antigens other than vaccine antigens). While this delay previously-observed in vaccine-based SIV controllers [10] can be explained not only by immunodominance but also by reduction in viral loads, the delay in vaccinated non-controllers in the present study might reflect the immunodominance in CTL responses. Thus, in development of a prophylactic, CTL-inducing AIDS vaccine, it is important to select vaccine antigens leading to effective CTL responses post-viral

exposure [21,22]. These results imply a significant influence of prophylactic vaccination on the immunodominance pattern of CTL responses post-viral exposure, providing insights into antigen design in development of a CTL-inducing AIDS vaccine.

## Acknowledgments

This work was supported by Grants-in-aid from the Ministry of Education, Culture, Sports, Science, and Technology, Grants-in-aid from the Ministry of Health, Labor, and Welfare, and a Grant from Takeda Science Foundation in Japan.

## References

[1] R.A. Koup, J.T. Safrit, Y. Cao, C.A. Andrews, G. McLeod, W. Borkowsky, C. Farthing, D.D. Ho, Temporal association of cellular immune responses with the initial control of viremia in primary human immunodeficiency virus type 1 syndrome, J. Virol. 68 (1994) 4650–4655.
[2] P. Borrow, H. Lewicki, B.H. Hahn, G.M. Shaw, M.B. Oldstone, Virus-specific CD8+ cytotoxic T-lymphocyte activity associated with control of viremia in primary human immunodeficiency virus type 1 infection, J. Virol. 68 (1994) 6103–6110.
[3] T. Matano, R. Shibata, C. Siemon, M. Connors, H.C. Lane, M.A. Martin, Administration of an anti-CD8 monoclonal antibody interferes with the clearance of chimeric simian/human immunodeficiency virus during primary infections of rhesus macaques, J. Virol. 72 (1998) 164–169.
[4] X. Jin, D.E. Bauer, S.E. Tuttleton, S. Lewin, A. Gettie, J. Blanchard, C.E. Irwin, J.T. Safrit, J. Mittler, L. Weinberger, L.G. Kostrikis, L. Zhang, A.S. Perelson, D.D. Ho, Dramatic rise in plasma viremia after CD8(+) T cell depletion in simian immunodeficiency virus-infected macaques, J. Exp. Med. 189 (1999) 991–998.
[5] P.J. Goulder, D.I. Watkins, HIV and SIV CTL escape: implications for vaccine design, Nat. Rev. Immunol. 4 (2004) 630–640.
[6] T. Matano, M. Kano, H. Nakamura, A. Takeda, Y. Nagai, Rapid appearance of secondary immune responses and protection from acute CD4 depletion after a highly pathogenic immunodeficiency virus challenge in macaques vaccinated with a DNA prime/Sendai virus vector boost regimen, J. Virol. 75 (2001) 11891–11896.
[7] T. Matano, M. Kobayashi, H. Igarashi, A. Takeda, H. Nakamura, M. Kano, C. Sugimoto, K. Mori, A. Iida, T. Hirata, M. Hasegawa, T. Yuasa, M. Miyazawa, Y. Takahashi, M. Yasunami, A. Kimura, D.H. O'Connor, D.I. Watkins, Y. Nagai, Cytotoxic T lymphocyte-based control of simian immunodeficiency virus replication in a preclinical AIDS vaccine trial, J. Exp. Med. 199 (2004) 1709–1718.
[8] Y. Takahashi-Tanaka, M. Yasunami, T. Naruse, K. Hinohara, T. Matano, K. Mori, M. Miysazawa, M. Honda, Y. Yasutomi, Y. Nagai, A. Kimura, Reference strand-mediated conformation analysis (RSCA)-based typing of multiple alleles in the rhesus macaque MHC class I Mamu-A and Mamu-B loci, Electrophoresis 28 (2007) 918–924.
[9] M. Kawada, T. Tsukamoto, H. Yamamoto, N. Iwamoto, K. Kurihara, A. Takeda, C. Moriya, H. Takeuchi, H. Akari, T. Matano, Gag-specific cytotoxic T lymphocyte-based control of primary simian immunodeficiency virus replication in a vaccine trial, J. Virol. 82 (2008) 10199–10206.
[10] T. Tsukamoto, A. Takeda, T. Yamamoto, H. Yamamoto, M. Kawada, T. Matano, Impact of cytotoxic-T-lymphocyte memory induction without virus-specific CD4+ T-Cell help on control of a simian immunodeficiency virus challenge in rhesus macaques, J. Virol. 83 (2009) 9339–9346.
[11] H. Yamamoto, M. Kawada, A. Takeda, H. Igarashi, T. Matano, Post-infection immunodeficiency virus control by neutralizing antibodies, PLoS ONE 2 (2007) e540.
[12] R. Shibata, F. Maldarelli, C. Siemon, T. Matano, M. Parta, G. Miller, T. Fredrickson, M.A. Martin, Infection and pathogenicity of chimeric simian-human immunodeficiency viruses in macaques: determinants of high virus loads and CD4 cell killing, J. Infect. Dis. 176 (1997) 362–373.
[13] H.O. Li, Y.F. Zhu, M. Asakawa, H. Kuma, T. Hirata, Y. Ueda, Y.S. Lee, M. Fukumura, A. Iida, A. Kato, Y. Nagai, M. Hasegawa, A cytoplasmic RNA vector derived from nontransmissible Sendai virus with efficient gene transfer and expression, J. Virol. 74 (2000) 6564–6569.
[14] A. Takeda, H. Igarashi, H. Nakamura, M. Kano, A. Iida, T. Hirata, M. Hasegawa, Y. Nagai, T. Matano, Protective efficacy of an AIDS vaccine, a single DNA priming followed by a single booster with a recombinant replication-defective Sendai virus vector, in a macaque AIDS model, J. Virol. 77 (2003) 9710–9715.
[15] H.W. Kestler 3rd, D.J. Ringler, K. Mori, D.L. Panicali, P.K. Sehgal, M.D. Daniel, R.C. Desrosiers, Importance of the nef gene for maintenance of high virus loads and for development of AIDS, Cell 65 (1991) 651–662.
[16] T. Matano, M. Kano, T. Odawara, H. Nakamura, A. Takeda, K. Mori, T. Sato, Y. Nagai, Induction of protective immunity against pathogenic simian immunodeficiency virus by a foreign receptor-dependent replication of an engineered avirulent virus, Vaccine 18 (2000) 3310–3318.
[17] L.M. Albritton, L. Tweng, D. Scadden, J.M. Cunningham, A putative murine retrovirus receptor gene encodes a multiple membrane-spanning protein and confers susceptibility to virus infection, Cell 57 (1989) 659–666.
[18] M. Kawada, T. Tsukamoto, H. Yamamoto, A. Takeda, H. Igarashi, D.I. Watkins, T. Matano, Long-term control of simian immunodeficiency virus replication with central memory CD4+ T-cell preservation after nonsterile protection by a cytotoxic T-lymphocyte-based vaccine, J. Virol. 81 (2007) 5202–5211.
[19] N. Iwamoto, T. Tsukamoto, M. Kawada, A. Takeda, H. Yamamoto, H. Takeuchi, T. Matano, Broadening of CD8+ cell responses in vaccine-based simian immunodeficiency virus controllers, AIDS 24 (2010) 2777–2787.
[20] S. Tenzer, E. Wee, A. Burgevin, G. Stewart-Jones, L. Friis, K. Lamberth, C.H. Chang, M. Harndahl, M. Weimershaus, J. Gerstoft, N. Akkad, P. Klenerman, L. Fugger, E.Y. Jones, A.J. McMichael, S. Buus, H. Schild, P. van Endert, A.K. Iversen, Antigen processing influences HIV-specific cytotoxic T lymphocyte immunodominance, Nat. Immunol. 10 (2009) 636–646.
[21] P.J.R. Goulder, D.I. Watkins, Impact of MHC class I diversity on immune control of immunodeficiency virus replication, Nat. Rev. Immunol. 8 (2008) 619–630.
[22] H. Streeck, J.S. Jolin, Y. Qi, B. Yassine-Diab, R.C. Johnson, D.S. Kwon, M.M. Addo, C. Brumme, J.P. Routy, S. Little, H.K. Jessen, A.D. Kelleher, F.M. Hecht, R.P. Sekaly, E.S. Rosenberg, B.D. Walker, M. Carrington, M. Altfeld, Human immunodeficiency virus type 1-specific CD8+ T-cell responses during primary infection are major determinants of the viral set point and loss of CD4+ T cells, J. Virol. 83 (2009) 7641–7648.
[23] L. Alexander, L. Denekamp, S. Czajak, R.C. Desrosiers, Suboptimal nucleotides in the infectious, pathogenic simian immunodeficiency virus clone SIVmac239, J. Virol. 75 (2001) 4019–4022.

Immunogenetics (2011) 63:501–509
DOI 10.1007/s00251-011-0531-y

ORIGINAL PAPER

# *ULBP4/RAET1E* is highly polymorphic in the Old World monkey

**Taeko K. Naruse · Yukiko Okuda · Kazuyasu Mori · Hirofumi Akari · Tetsuro Matano · Akinori Kimura**

Received: 22 February 2011 / Accepted: 21 April 2011 / Published online: 7 May 2011


**Abstract** Natural-killer group 2 member D (NKG2D) is an activating receptor that plays an important role in the immune response mediated by NK cells, $\gamma\delta^+$ T cells, and $CD8^+$ T cells. In humans, MHC class I chain-related genes and UL-16 binding protein (ULBP)/retinoic acid early transcript 1 (REAT1) gene family encode ligands for NKG2D. The rhesus and crab-eating macaques, which belong to the Old World monkeys, are widely used as non-human primate models in medical researches on the immunological process. In the present study, we investigated the polymorphisms of *ULBP4/RAET1E*, a member of the *ULBP/RAET1* family, and found 25 and 14 alleles from the rhesus and crab-eating macaques, respectively, of which diversities were far more extended than in humans. A phylogenetic study suggested that the allelic diversification of ULBP4/RAET1E predated the divergence of rhesus and crab-eating macaques.

T. K. Naruse · A. Kimura (✉)
Department of Molecular Pathogenesis, Medical Research Institute, Tokyo Medical and Dental University,
1-5-45 Yushima, Bunkyo-ku,
Tokyo 113–8510, Japan
e-mail: akitis@mri.tmd.ac.jp

Y. Okuda · A. Kimura
Laboratory of Genome Diversity, Graduate School of Biomedical Science, Tokyo Medical and Dental University,
Tokyo, Japan

K. Mori · T. Matano
AIDS Research Center, National Institute of Infectious Diseases,
Tokyo, Japan

H. Akari
Primate Research Institute, Kyoto University,
Inuyama, Japan

T. Matano
International Research Center for Infectious Diseases,
The Institute of Medical Science, The University of Tokyo,
Tokyo, Japan

**Keywords** Rhesus macaque · Crab-eating macaque · ULBP4/RAET1E · NKG2D · Polymorphism

## Introduction

Non-human primates, such as rhesus and crab-eating macaques, are important animal models for the study of infectious diseases, autoimmune diseases, and organ transplantation. These macaques are members of the Old World monkeys, and it has been reported that the genetic diversity in the rhesus macaque is quite unique, that is, more than 60% of the rhesus macaque-specific expansions are found in the protein coding sequences (Gibbs et al. 2007). To evaluate the results of immunological experiments in the macaque models, it is essential to characterize the genetic diversity of immune-related molecules which may control the individual differences in the immune response against foreign antigens and/or pathogens. It has been reported that the gene copy number in the major histocompatibility complex (MHC) loci in the rhesus and crab-eating macaques is higher than that in humans (Kulski et al. 2004; Gibbs et al. 2007; Otting et al. 2007). In addition, the extent of genetic diversity differed, in part, depending on the geographic areas, and we have reported that the diversity of MHC class I genes in the rhesus macaque is considerably different depending on habitat (Naruse et al. 2010).

Because the innate immune system is involved in the response to environmental pathogens, it is necessary to consider the function of natural killer (NK) cells in the experimental animal models. Natural-killer group 2 member D (NKG2D), a C-type lectin molecule, is an activating receptor expressed on the cell surface of NK, $\gamma\delta^+$, and $CD8^+$ T cells, which plays an important role in the immune response (Wu et al. 1999; Raulet 2003). In humans, MHC class I chain-related genes (MIC) and UL-16 binding protein (ULBP)/retinoic acid early transcript 1 (REAT1)

gene family are known to encode ligands for NKG2D (Bauer et al. 1999; Cosman et al. 2001; Chalupny et al. 2003; Bacon et al. 2004). These ligand molecules are usually stress-inducible, and their recognition by NKG2D can lead to the activation of NK cells, consequently killing virus-infected and tumor cells (Pende et al. 2002; Eagle et al. 2006; Pappworth et al. 2007; Ward et al. 2007).

The human *ULBP/RAET1* gene family is located on chromosome 6q24.2, which is composed of ten members including six functional genes, *ULBP1*, *2*, *3*, *4*, *5*, and *6*, corresponding to *RAET1I*, *H*, *N*, *E*, *G*, and *L*, respectively (Radosavljevic et al. 2001; Chalupny et al. 2003; Eagle et al. 2009a, b). In addition, several sequence polymorphisms in each *ULBP* gene have been identified (Romphruk et al. 2009; Antoun et al. 2010). Although it is evident that the cell surface expression of the ligand molecules on target cells is differentially regulated (Eagle et al. 2006), genetic polymorphisms in the coding regions might have a functional impact. We have previously investigated the genetic polymorphisms of *ULBP/RAET1* genes and have found that the *ULBP4/RAET1E* gene is the most polymorphic, with the allelic distribution differing among ethnic groups (Romphruk et al. 2009).

On the other hand, rhesus macaque *ULBP4/RAET1E* (GenBank: NW_001116520) is mapped on the long arm of chromosome 4 (i.e., positions from 31, 164, 822 to 31, 175, 032 of chromosome 4 in the rhesus genome; data obtained from the UCSC Genome Browser at http://genome.ucsc.edu/cgi-bin/hgGateway; Gibbs et al. 2007). However, its genetic polymorphisms are poorly characterized, although the MIC gene polymorphisms are well studied in the rhesus macaque (Seo et al. 1999, 2001; Doxiadis et al. 2007; Averdam et al. 2007). In the present study, we investigated the polymorphisms of *ULBP4/RAET1E* in rhesus and crab-eating macaques. This is the first report demonstrating the extreme diversity of the NKG2D ligand in the Old World monkey.

## Materials and methods

### Animals

A total of 38 rhesus macaques from seven lineages previously analyzed for the MHC polymorphisms (Naruse et al. 2010) and 24 crab-eating macaques from five lineages were the subjects. They were maintained in the breeding colonies in Japan. The founders of the rhesus macaque colonies were captured in Myanmar and Laos, whereas the founders of crab-eating macaque colonies were captured in Indonesia, Malaysia, and the Philippines. All care, including blood sampling of animals, were in accordance with the guidelines for the Care and Use of Laboratory Animals published by the National Institutes of Health (NIH publication 85–23, revised 1985) and were subjected to prior approval by the local animal protection authority.

### DNA extraction and sequencing analysis

Genomic DNAs from B lymphoblastoid cell lines of the rhesus macaque (Naruse et al. 2010) and from whole blood sample of the crab-eating macaque were extracted by using the QuickGene DNA kit (Fujifilm, Tokyo, Japan) according to the manufacturer's instructions. The genomic gene for *ULBP4/RAET1E* of rhesus and crab-eating macaques was amplified by polymerase chain reaction (PCR) with a primer pair designed for the region spanning from introns 1 to 3 of the rhesus gene (NC007861), ULBP4F (5′-TGGGCCTCTTCCCCTGTCC) and ULBP4R (5′-GTGGGAGGTGGGATGGG), using FastStart Taq DNA polymerase (Roche, Mannheim, Germany). The PCR condition was composed of the following steps: denaturation at 95°C for 4 min; 30 cycles of 95°C for 30 s, 63°C for 30 s, and 72°C for 45 s; and additional extension at 72°C for 7 min. The PCR products of about 1,200 bp in length were cloned into pSTBlue-1 AccepTer vector (Novagen, WI, USA) according to the manufacturer's instructions and were transformed to Nova Blue Single™ competent cells (Merck4Biosciences Japan, Tokyo, Japan). Ten to 20 independent transformant colonies were picked up for each sample and subjected to sequencing on both strands by using a BigDye Terminator cycling system and an ABI 3730 automated sequence analyzer (Applied Biosystems, CA, USA).

### Data analyses

Nucleotide sequences of *ULBP4/RAET1E* from cloned DNAs were aligned using the Genetyx software package (version 8.0, Genetyx Corp., Japan). If at least three clones from independent PCR or from different individuals showed identical sequences, the sequences were submitted to the DNA Data Bank of Japan (DDBJ). Neighbor-joining trees were constructed with Kimura's 2-parameter method for a phylogenetic analysis of *ULBP4/RAET1E* sequences spanning from exons 2 to 3 including intron 2 by using the Genetyx software. Bootstrap values were based on 5,000 replications. The *ULBP4/RAET1E* sequences from humans (GenBank accession number AY252119), chimpanzees (AY032638), and rhesus (NC007861) were included in the analysis as references.

### Structure model analysis

A three-dimensional (3-D) structure model of rhesus ULBP4/RAET1E, with amino acid positions from 1 to 178, was created by a molecular visualization software RasTop2.2 (http://sourceforge.net/projects/rastop/), and the

human RAET1B in complex with NKG2D (Radaev et al. 2001) from the Molecular Modeling Database (MMCB No. 18231) was used as the reference. Polymorphic sites were mapped on the 3-D structure model of macaque RAET1E by using the Cn3D 4.1 program (http://www.ncbi.nlm.nih.gov/Structure/CN3D/cn3d.shtml).

**Table 1** Identified alleles of the ULBP4 gene in rhesus and cynomolgus

| Species | Allele name | Accession no. | Reference animal | Identical sequence |
|---|---|---|---|---|
| Rhesus macaque | *Mamu-ULBP4*1.1* | AB568525 | R228, R367 | |
| | *Mamu-ULBP4*1.2* | AB568533 | R492, R396, R465 | |
| | *Mamu-ULBP4*2* | AB568526 | R283, R384, R328, R337 | |
| | *Mamu-ULBP4*3* | AB568527 | R346, R361, R396, R379, R408 | |
| | *Mmau-ULBP4*4* | AB568528 | R320, R490, R321, R465, R367, R446, R328, R234, R237, R314 | |
| | *Mamu-ULBP4*5* | AB568529 | R430, R453, R325, R477, R439, R360, R379, R446, R355 | |
| | *Mamu-ULBP4*6* | AB568530 | R437, R350, | |
| | *Mamu-ULBP4*7.1* | AB568531 | R325, R384, R491, R333, R337 | |
| | *Mamu-ULBP4*7.2* | AB568544 | R477 | |
| | *Mamu-ULBP4*8* | AB568532 | R408, R454, R241, R342, R316 | |
| | *Mamu-ULBP4*9.1* | AB568534 | R312, R314 | |
| | *Mamu-ULBP4*9.2* | AB568535 | R333 | |
| | *Mamu-ULBP4*10* | AB568536 | R316 | |
| | *Mamu-ULBP4*11* | AB568537 | R241 | |
| | *Mamu-ULBP4*12* | AB568538 | R342 | |
| | *Mamu-ULBP4*13* | AB568539 | R491 | |
| | *Mamu-ULBP4*14* | AB568540 | R495 | *Mafa-ULBP4*1.1* |
| | *Mamu-ULBP4*15* | AB568541 | R350 | |
| | *Mamu-ULBP4*16* | AB568542 | R492 | |
| | *Mamu-ULBP4*17* | AB568543 | R495 | |
| | *Mamu-ULBP4*18* | AB568545 | R454 | |
| | *Mamu-ULBP4*19* | AB568546 | R321 | |
| | *Mamu-ULBP4*20* | AB568547 | R355 | |
| | *Mamu-ULBP4*21* | AB571025 | R437 | |
| | *Mamu-ULBP4*22* | AB571026 | R439 | |
| Crab-eating macaque | *Mafa-ULBP4*1.1* | AB578934 | M01, P01, P02, C001, C003, C004, C005, C006 | *Mamu-ULBP4*14* |
| | *Mafa-ULBP4*1.2* | AB578935 | M02, C004 | |
| | *Mafa-ULBP4*2* | AB578936 | P04, M06, C010, C011, C013 | |
| | *Mafa-ULBP4*3* | AB578938 | M03, C007 | |
| | *Mafa-ULBP4*4* | AB578939 | M03, C006 | |
| | *Mafa-ULBP4*5* | AB578940 | P04, P05, M05, M06, C012, C013 | |
| | *Mafa-ULBP4*6* | AB578941 | M05, C010, C011 | |
| | *Mafa-ULBP4*7.1* | AB578942 | M01, C002 | |
| | *Mafa-ULBP4*7.2* | AB578943 | P03, C008 | |
| | *Mafa-ULBP4*8* | AB578944 | P03, M04, C008, C009 | |
| | *Mafa-ULBP4*9* | AB578945 | P01, C001, C002 | |
| | *Mafa-ULBP4*10* | AB578946 | M04, C009 | |
| | *Mafa-ULBP4*11* | AB578947 | P02, C007 | |
| | *Mafa-ULBP4*12* | AB578948 | M02, C005 | |

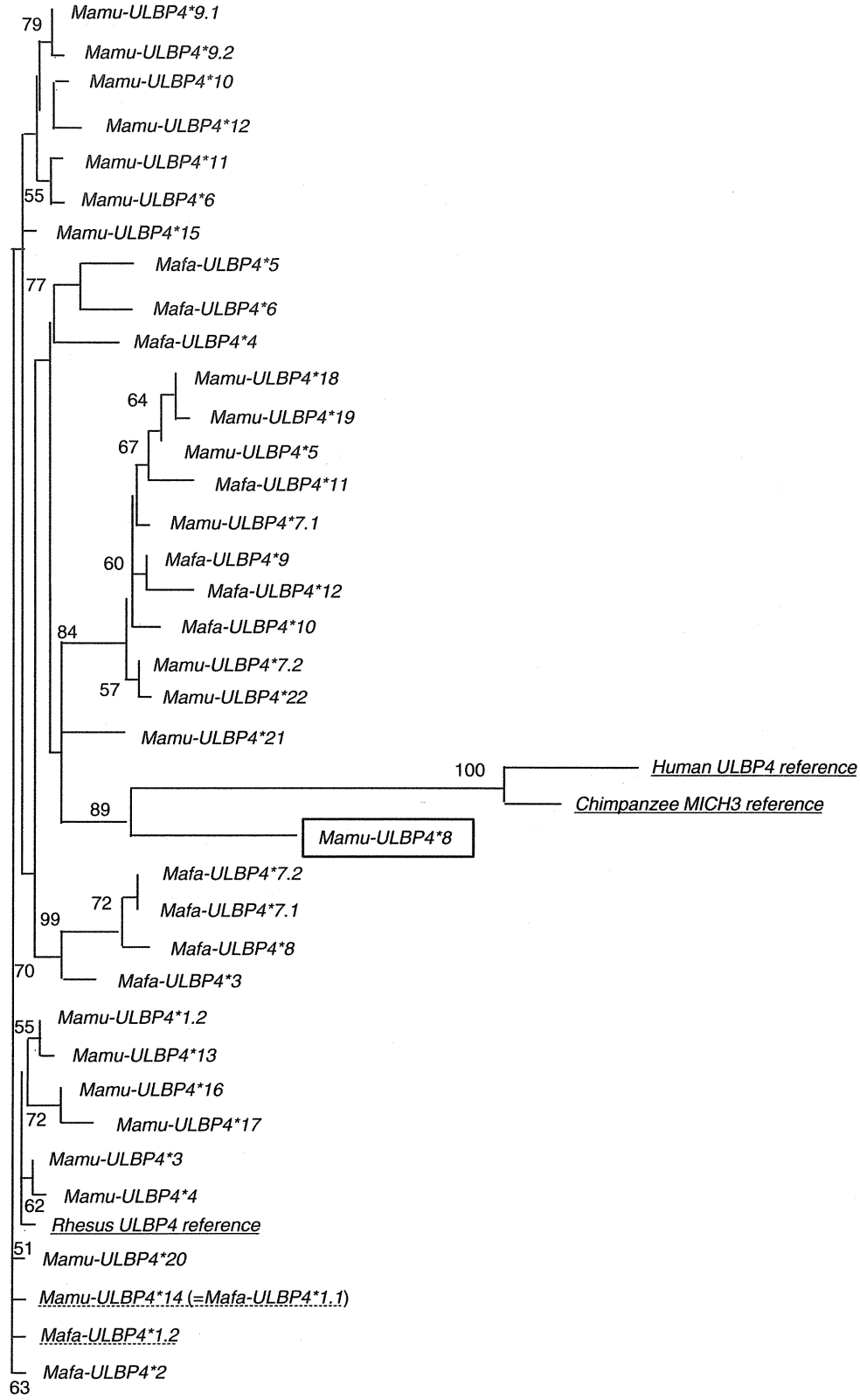


**Fig. 1** Phylogenetic tree of *Mamu-* and *Mafa-ULBP4/RAET1E* alleles. A phylogenetic tree of *ULBP4/RAET1E* sequences spanning from exons 2 to 3, obtained in this study, was constructed by using the neighbor-joining method with bootstrap values of 5,000 replications. Values are indicated as percentages, and only those with more than 50% are shown. Sequences of human *ULBP4/RAET1E* (AY252119), chimpanzee *MICH3* (AY032638), and rhesus *ULBP4/RAET1E* (NC007861) were *underlined* and included in the analysis as reference sequences. Alleles represented with *broken underlines* had identical amino acid sequences predicted from the nucleotide sequences. The allele containing an in-frame termination codon was *boxed*

## Results

### *ULBP4/RAET1E* polymorphisms in the rhesus macaque

In the rhesus macaque genome (Gibbs et al. 2007), there are two paralogous genes for *ULBP4/RAET1E*, one of which appears to be functional, whereas the other is a pseudogene because it contains a large deletion containing the most part of exons 2, 3, and 4. Therefore, we designed primer pairs to amplify the region containing exons 2 and 3, which encode for α1 and α2 domains of ULBP4/RAET1E molecule, respectively, from the functional *ULBP4/RAET1E*. By using the primer pair, we obtained *ULBP4/RAET1E* sequences from 38 individuals of rhesus macaque. Because one or two sequences were obtained from each individual, the sequences were considered to be alleles of *ULBP4/RAET1E*. They were classified into 25 different alleles, designated as *Mamu-ULBP4*1.1* to *Mamu-ULBP4*22*, submitted to DDBJ, and given accession numbers (Table 1). The allele names with different numbers indicate that they are different in predicted amino acid sequences, whereas the alleles with the same deduced amino acid sequences but different nucleotide sequences, such as *Mamu-ULBP4*1.1* and *Mamu-ULBP4*1.2*, are designated as subtypes. None of the sequences obtained in this study was identical to the reference sequence, NC007861, which was previously deposited to the GenBank database as the rhesus *ULBP4/RAET1E*. On the other hand, when the sequences were aligned referring the human *ULBP4/RAET1E*, one rhesus allele (*Mamu-ULBP4*8*) was found to contain a nonsense mutation at codon 29, which would make the ULBP4/RAET1E molecule non-functional.

### *ULBP4/RAET1E* polymorphisms in the crab-eating macaque

By using the primer pair designed for the rhesus *ULBP4/RAET1E*, we could amplify the *ULBP4/RAET1E* sequences from 24 individuals of the crab-eating macaque. Sequencing analysis revealed 14 different *ULBP4/RAET1E* alleles, and inheritance of each allele was confirmed by family studies. The identified allele sequences were submitted to DDBJ, given accession numbers, and designated as *Mafa-ULBP4*1.1* to *Mafa-ULBP4*12* (Table 1). The nucleotide sequences from exons 2 to 3 of *Mamu-ULBP4*14* were identical to those of *Mafa-ULBP4*1.1* and differed by only one nucleotide in intron 2 from those of *Mafa-ULBP4*1.2*. In addition, a neighbor-joining analysis performed by using nucleotide sequences spanning from exons 2 to 3 showed that the alleles of rhesus and crab-eating macaques were not separately clustered from each other (Fig. 1).

### Comparative analysis of *ULBP4/RAET1E*

The alignment of *ULBP4/RAET1E* sequences from rhesus and crab-eating macaques with those from humans and chimpanzees showed that the macaque genes were homologous to the human gene by more than 90% and were equally diverged (Fig. 2). In addition, rhesus and crab-

```
                                                                                50
                Human :GHSLCFNFTI KSLSRPGQPW CEAQVFLNKN LFLQYNSDNN MVKPLGLLGK KVYATSTwge
            Chimpanzee :---------- -L-------- ---------- ---------- ---------- --N-------
      Rhesus macaque   :A--------- --W------- ------M-K- -----D—S- ---------- --N-----Q-
Crab-eating macaque    :A--------- --W------- ------M--- -F---D—SN ---------- --N-----Q-

                                                                    100
                Human :ltqtlgevgr dlrmllcdIK PQIKTSDPST LQVEMFCQRE AERCTGASWQ FATNGEKSLL
            Chimpanzee :---M------ ------L--- ------G--- ---------- ---------- --I-------
      Rhesus macaque   :---K------ ------L-V- ------GP-- -----L---- ---------- -TI----C--
Crab-eating macaque    :---------- -LM---L-V- P-----G--- L----L---- ---------- -TI----C--

                                                          150
                Human :FDAMNMTWTV INHEAskike twkkdrglek yfrklskgdc dhwlreflgh weampEPTV
            Chimpanzee :---------- ---------- ---------- ---------- ---------- --------Q
      Rhesus macaque   :F----M---- ----AS---- ---K------ ------M--- N------L-- Q-A-----Q
Crab-eating macaque    :---------- -----S---- ---------- ------M--- N-WLR----- Q------TQ
```

**Fig. 2** Alignment of deduced amino acid sequences of α1 and α2 domains of ULBP4/RAET1E. Amino acid sequences were deduced from the nucleotide sequences of *ULBP4/RAET1E* or *MICH3* from humans (AY252119), chimpanzees (AY032638), rhesus macaques (NC007861), and crab-eating macaques (AY032639). *Numbers* above the sequences represent the amino acid positions in mature protein. *Dashes* indicate identical sequences. Sequences for the predicted α helix structure were indicated by *small italicized characters*. Positions of polymorphic sites in the *human*, *rhesus macaque*, and *crab-eating macaque* were *underlined*

**Table 2** Single nucleotide polymorphisms of ULBP4 gene among human and Old World monkeys

| | Number of alleles | Exon 2 | | Intron 2 | Exon 3 | |
|---|---|---|---|---|---|---|
| | | Polymorphism | Non-synonymous change (%) | Polymorphism | Polymorphism | Non-synonymous change (%) |
| Human | 5 | 2 | 2 (100%) | 3 | 3 | 3 (100%) |
| Rhesus macaque | 25 | 9 | 5 (55.6%) | 22 | 22 | 14 (63.6%) |
| Crab-eating macaque | 14 | 17 | 9 (52.9%) | 18 | 16 | 9 (56.3%) |

eating macaques showed a higher degree of polymorphism in the analyzed region, namely, exon 2, intron 2, and exon 3, than in humans (Table 2). All polymorphisms found in exons of human *ULBP4/RAET1E* were non-synonymous, whereas a considerable part of the polymorphisms were synonymous in the Old World monkeys. On the other hand, the polymorphic sites in the rhesus macaque (positions 29, 46, 59, 64, 79, 88, 112, 121, 126, 135, 136, 144, 157, 158, 161, 168, 171, and 173) and the crab-eating macaque (positions 32, 39, 40, 59, 72, 73, 79, 91, 112, 136, 163, 164, 165, 171, 178, and 179) were shared at five positions (59, 79, 112, 136, and 171) by each other, whereas only one position (position 112) was shared with polymorphic sites in humans (positions 53, 99, 112, and 113) (Fig. 2). In addition, a termination at position 29 was found in a rhesus macaque allele *Mamu-ULBP4*8*; a single amino acid deletion caused by deletions of a total of three nucleotides was found in a crab-eating macaque allele *Mafa-ULBP4*6* [i.e., TGGCTCAGG sequences corresponding to codons 163–165 were changed to TGCTCA, which may be due to two different deletions at codons 163 (from TGG to TG) and 165 (from AGG to A)], whereas such polymorphisms were not observed in humans. These findings suggest that a selection pressure to generate and maintain the polymorphic sites might be considerably different between the lineages of humans and the Old World monkeys.

## Discussion

It has been suggested that the ancestral gene for the ULBP/REAT molecule of placental mammals was originally diverged and duplicated in each species after an emigration from the MHC region (Kondo et al. 2010). In humans, MHC genes (*HLA* genes) are clustered and mapped on the short arm of chromosome 6, 6p21.3, whereas the *ULBP/RAET1* genes are located on the long arm of chromosome 6, 6q25.1. As for the *MHC* genes in the macaque, it was previously reported that rhesus macaque MHC, e.g., BAT1 gene, was localized to chromosome 6q24 by using fiber-fluorescence in situ hybridization (Huber et al. 2003) and cynomolgus (crab-eating) macaque MHC, e.g., Mafa-A and Mafa-B genes, was cytogenetically mapped to chromosome 6p13 (Liu et al. 2007), although the rhesus macaque MHC is mapped on the short arm of chromosome 4 in the draft genome sequence database of rhesus macaques (Gibbs et al. 2007); e.g., Mamu-A and BAT1 were mapped from positions 29, 517, 308 to 29, 520, 221 and from 31, 164, 822 to 31, 175, 032, respectively, on chromosome 4 (data were obtained from the UCSC Genome Browser at http://genome.ucsc.edu/cgi-bin/hgGateway). The discrepancy between the cytogenetic mapping and the assignment in draft genome sequence should be resolved in the future. On the other hand, it is interesting to note that each member of the *ULBP/RAET1* gene family, except for *ULBP6*, is completely or partially duplicated in the rhesus genome. As for the *ULBP4/RAET1E*, two related sequences, LOC695031 (NC007861) and LOC694265, have been identified as orthologs of human *ULBP4/RAET1E*. On the other hand, the configuration of *ULBP/RAET1* loci in the crab-eating macaque genome remained unknown. Because LOC694265 was a pseudogene lacking most part of the coding exons, we designed PCR primers by referring the NC007861 sequence. By using the designed primers, we could successfully amplify *ULBP4/RAET1E* alleles from both rhesus and crab-eating macaques.

In this study, we identified a total of 25 and 14 alleles from rhesus and crab-eating macaques, respectively. One of the rhesus macaque alleles had identical sequences to one of the crab-eating macaque alleles, and the phylogenetic analysis demonstrated that the *ULBP4/RAET1E* alleles were widely diverged. None of the alleles identified in this study were identical to the previously reported sequence NC007861, which was derived from an individual of Indian rhesus macaque. Given that we analyzed rhesus macaques of Burmese origin in this study, and allele distribution of MHC-related polymorphic genes are well known to be largely dependent on the habitat regions, the extent of diversity and variation in *ULBP4/RAET1E* may be further expanded.

It was demonstrated that the diversity of *ULBP4/RAET1E* in the Old World monkeys was much higher than that of human *ULBP4/RAET1E*. It is possible that the genes in the *ULBP/RAET1* locus, in particular, *ULBP4/RAET1E* and *ULBP/RAET1*s, might be highly polymorphic in the

Old World monkeys. We therefore investigated ten unrelated rhesus macaque subjects, in which we had detected 16 *ULBP4/RAET1E* alleles for polymorphisms in the adjacent *ULBP/RAET1* genes. We found one *ULBP1/RAET1I* allele, seven *ULBP2/RAET1H* alleles, and one *ULBP3/RAET1N* allele in these subjects. The observation suggested that *ULBP4/RAET1E* was highly polymorphic as compared to the adjacent *ULBP/RAET1* genes.

We revealed a high degree of polymorphism in the *ULBP4/RAET1E* of the rhesus and crab-eating macaques, although about half of the polymorphisms were synonymous changes (Table 2). Albeit the expression of the ULBP4/RAET1E molecule is known to be involved in the recognition of tumor cells by the NKG2D receptor (Cao et al. 2008; Kong et al. 2009), the functional significance of the polymorphisms in the extracellular domain of the ULBP4/RAET1E molecules remained unknown. To investigate a possible role of the polymorphisms, we have created a 3-D structure model of rhesus ULBP4/RAET1E molecule by using the structure data of human ULBP3/RAET1N in complex with NKG2D (Radaev et al. 2001) as the reference. As shown in Fig. 3, only one polymorphic site at 173 was on the surface of the α helix pointing to the NKG2D receptor, five sites at 59, 136, 144, 161, and 165 were positioned outside the α helix, and only two sites at 32 and 91 were mapped on the β sheet in the groove. The other polymorphic sites were on the β sheet outside of the groove or were not on the surface of the α helix. In addition, expression of *ULBP4/RAET1E* is predominantly found in the skin and tumor tissues and not induced by viral infection in normal cells (Chalupny et al. 2003; Eagle et al. 2006). These observations suggest that the polymorphisms are unlikely to be involved in the differential presentation of characteristic small molecules bound by the ULBP4/RAET1E molecules, as found in the presentation of antigenic peptides by the MHC molecules. Nevertheless, highly prevalent polymorphisms leading to amino acid replacements suggest that a selection pressure had operated on the configuration of diversity in *ULBP4/RAET1E*.

Of particular interest in this study was the rhesus macaque allele *Mamu-ULBP4*8*, which was supposed to contain a stop codon in the exon 2 coding sequence that would truncate the most part of the molecule. This is the first report of a non-functional *ULBP/RAET1* allele in primates; however, a similar situation was reported for another NKG2D ligand gene, *MIC*. For example, a specific human *MIC* haplotype linked to HLA-B*048 consists of non-functional *MIC* genes, in which *MICA* was deleted and *MICB* contained a termination codon (Ota et al. 2000); the non-functional *MIC* haplotype is widely distributed in the East Asian populations (Komatsu-Wakui et al. 2001). It is interesting to note that there are two distinct and polymorphic genes for *MIC* in the rhesus macaque, *MICA* (previously designated as *MIC1* and *MIC3*) and *MICB* (previous *MIC2*); however, they are not considered to be orthologous to the human *MICA* and *MICB* genes, respectively (Seo et al. 1999, 2001; Doxiadis et al. 2007; Averdam et al. 2007). Because members of the MIC and ULBP/RAET1 molecules are structurally related (Li et al. 2002), there is a functional redundancy in the recognition by NKG2D, and thus, the presence of a null allele had been allowed during the evolution of primates.

In the present study, we demonstrated the *ULBP4/RAET1E* allelic polymorphisms not only in the rhesus macaque but also in the crab-eating macaque. Although the localization of *ULBP4/RAET1E* in the crab-eating macaque

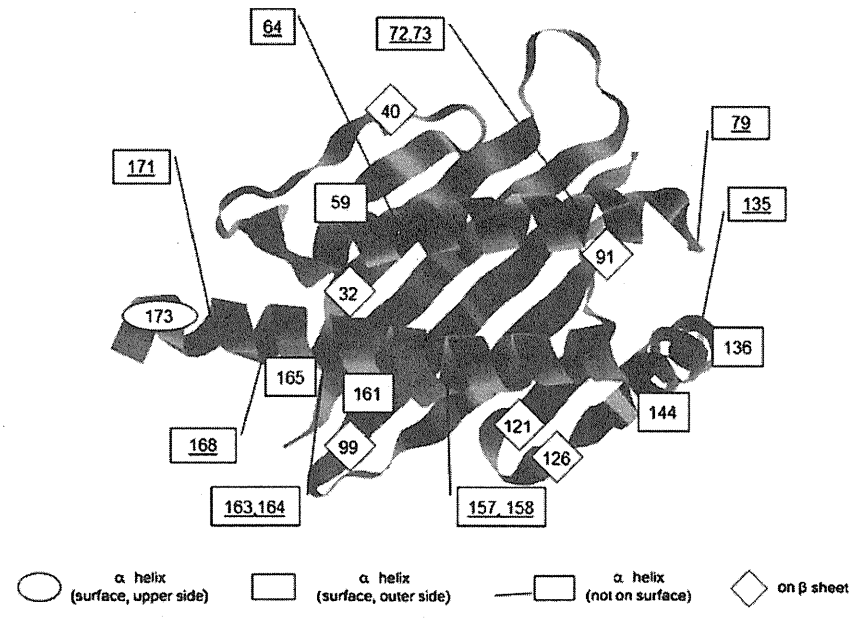


**Fig. 3** Mapping of polymorphic sites on the structure model of the macaque ULBP4/RAET1E molecule. Polymorphic sites found in the Old World monkeys were mapped on the 3-D structure model of ULBP4/RAET1E. Residues on the upper and outer sides of the α helix structure were indicated by a *circle* and *squares*, respectively. Residues not found on the surface of the α helix were *underlined*, and those on the β sheet structure were represented by *rhombi*

genome is unknown, a homology search showed that a *Mafa-MICH3* gene (AY032639) was homologous to *Mafa-ULBP4/RAET1E* because the nucleotide sequences of *Mafa-ULBP4*1.1* showed a 96% homology to *Mafa-MICH3*. Similarly, nucleotide sequences of a chimpanzee gene, *Patr-MICH3* (AY032638), showed a 94% homology to the rhesus *ULBP4/RAET1E*. These findings strongly suggest that *MICH3* in the crab-eating macaque and chimpanzee is orthologous to *ULBP4/RAET1E* in the human and rhesus macaque.

In conclusion, we revealed a large diversity of *ULBP4/RAET1E* in two related species of the Old World monkey. Because there were extremely large polymorphisms in the extracellular domain of the ULBP4/RAET1E molecule in the Old World monkey, which was larger than that in the human, the functional impact of the polymorphisms and its significance in the evolution of primates should be investigated in future studies.

**Acknowledgments** We thank Ms. Yukiko Ueda for her technical assistance. This work was supported, in part, by research grants from the Ministry of Health, Labor and Welfare, Japan; the Japan Health Science Foundation; the program of Founding Research Centers for Emerging and Reemerging Infection Disease; the program of Research on Publicly Essential Drugs and Medical Devices; grants-in-aid for scientific research from the Ministry of Education, Culture, Sports, Science, and Technology (MEXT), Japan; a support for women researchers from the Tokyo Medical and Dental University; and a grant from the Life Science Institute Foundation.

## References

Antoun A, Jobson S, Cook M, O'Callaghan CA, Moss P, Briggs DC (2010) Single nucleotide polymorphism analysis of the NKG2D ligand cluster on the long arm of chromosome 6: extensive polymorphisms and evidence of diversity between human populations. Hum Immunol 71:610–620

Averdam A, Seelke S, Grützner I, Ronser C, Roos C, Westphal N, Stahl-Hennig C, Muppala V, Schrod A, Sauermann U, Dressel R, Walter L (2007) Genotyping and segregation analyses indicate the presence of only two functional MIC genes in rhesus macaques. Immunogenetics 59:247–251

Bacon L, Eagle RA, Meyer M, Easom N, Young NT, Trowsdale J (2004) Two human ULBP/RAET1 molecules with transmembrane region are ligands for NKG2D. J Immunol 173:1078–1084

Bauer S, Groh V, Wu J, Steinle A, Phillips JH, Lanier LL, Spies T (1999) Activation of NK cells and T cells by NKG2D, a receptor for stress-inducible MICA. Science 285:727–729

Cao W, Xi X, Wang Z, Dong L, Hao Z, Cui L, Ma C, He W (2008) Four novel ULBP splice variants are ligands for human NKG2D. Int Immunol 20:981–991

Chalupny NJ, Sutherland CL, Lawrence WA, Rein-Weston A, Cosman D (2003) ULBP4 is a novel ligand for human NKG2D. Biochem Biophys Res Commun 305:129–135

Cosman D, Müllberg J, Sutherland CL, Chin W, Armitage R, Fanslow R, Kubin M, Chalupny NJ (2001) ULBPs, novel MHC class I–related molecules, bind to CMV glycoprotein UL16 and stimulate NK cytotoxicity through the NKG2D receptor. Immunity 14:123–133

Doxiadis GGM, Heijmans CM, Otting N, Bontrop RE (2007) MIC gene polymorphism and haplotype diversity in rhesus macaques. Tissue Antigens 69:212–219

Eagle RA, Traherne JA, Ashiru O, Wills MR, Trowsdale J (2006) Regulation of NKG2D ligand gene expression. Hum Immunol 67:1159–1169

Eagle RA, Flack G, Warford A, Martinez-Borra J, Jafferji I, Traherne JA, Ohashi M, Boyle LH, Barrow AD, Caillat-Zucman S, Young NT, Trowsdale J (2009a) Celllar expression, trafficking, and function of two isoforms of human ULBP5/RAET1G. Pros ONE 4:e4503

Eagle RA, Traherne JA, Hair JR, Jafferji I, Trowsdale J (2009b) ULBP6/RAET1L is an additional human NKG2D ligand. Eur J Immunol 39:3207–3216

Gibbs RA, Rogers J, Katze MG et al (2007) Evolutionary and biomedical insights from the rhesus macaque genome. Science 316:222–234

Huber I, Walter L, Wimmer R, Pasantes JJ, Günther E, Schempp W (2003) Cytogenetic mapping and orientation of the rhesus macaque MHC. Cytogenet Genome Res 103:144–1449

Komatsu-Wakui M, Tokunaga K, Ishikawa Y, Leelayuwat C, Kashiwase K, Tanaka H, Moriyama S, Nakajima F, Park MH, Jia GJ, Chimge NO, Sideltseva EW, Juji T (2001) Wide distribution of the MICA-MICB null haplotype in East Asians. Tissue Antigens 57:1–8

Kondo M, Maruoka T, Otsuka N, Kasamatsu J, Fugo K, Hanzawa N, Kasahara M (2010) Comparative genomic analysis of mammalian NKG2D ligand family genes provides insights into their origin and evolution. Immunogenetics 62:441–450

Kong Y, Cao W, Xi X, Ma C, Cui L, He W (2009) The NKG2D ligand ULBP4 binds to TCRgamma9/delta2 and induces cytotoxicity to tumor cells through both TCRgammadelta and NKG2D. Blood 114:310–317

Kulski JK, Anzai T, Shiina T, Inoko H (2004) Rhesus macaque class I duplicon structures, organization, and evolution within the alpha block of the major histocompatibility complex. Mol Biol Evol 21:2079–2091

Li P, McDermott G, Strong RK (2002) Crystal structures of RAE-1β and its complex with the activating immunoreceptor NKG2D. Immunity 16:77–86

Liu QY, Wang XX, Zhang JZ, Chen WH, He XW, Lin Y, Wang JF, Zhu Y, Hu SN, Wang XN (2007) Mapping cynomolgus monkey MHC class I district on chromosome 6p13 using pooled cDNAs. Biotech Histochem 82:267–272

Naruse KT, Chen Z, Yanagida R, Yamashita T, Saito Y, Mori K, Akari H, Yasutomi Y, Miyazawa M, Matano T, Kimura A (2010) Diversity of MHC class I genes in Burmese-origin rhesus macaque. Immunogenetics 62:601–611

Ota M, Bahram S, Katsuyama Y, Saito S, Nose Y, Sada M, Ando H, Inoko H (2000) On the MICA deleted-MICB null, HLA-B*4801 haplotype. Tissue Antigens 56:268–271

Otting N, Otting N, deVos-Rouweler AJM, Heijmans CMC, de Groot NG, Doxiadis GGM, Bontrop RE (2007) MHC class I A region diversity and polymorphism in macaque species. Immunogenetics 59:367–375

Pappworth IY, Wang EC, Rowe M (2007) The switch from latent to productive infection in Epstein-Barr virus-infected B cell is associated with sensitization to NK cell killing. J Virol 1:474–482

Pende D, Rivera P, Marcenaro S, Chang CC, Biassoni R, Conte R, Kubin M, Cosman D, Ferrone S, Moretta L, Moretta A (2002) Major histocompatibility complex class I-related chain A and UL16-binding protein expression on tumor cell lines of different histotypes: analysis of tumor susceptibility to NKG2D-dependent natural killer cell cytotoxicity. Cancer Res 62:6178–6186